iScience

CellPress
OPEN ACCESS

Article

Mitochondrial transplantation ameliorates doxorubicin-induced cardiac dysfunction via activating glutamine metabolism

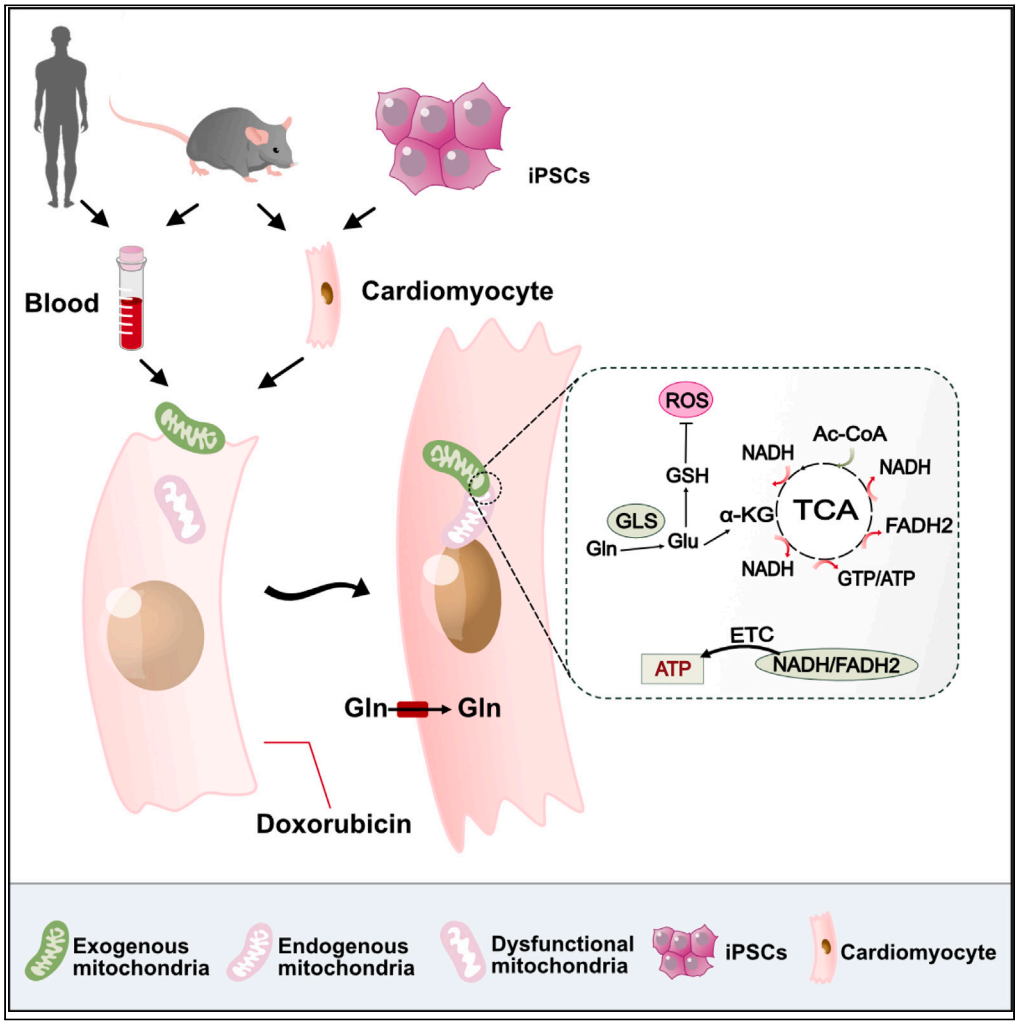

Xiaolei Sun, Hang Chen, Rifeng Gao, ..., Kai Hu, Junbo Ge, Aijun Sun

sun.aijun@zs-hospital.sh.cn

Highlights

Doxorubicin damages mitochondrial structure and function and results in cardiac injury

Mitochondrial transplantation inhibits doxorubicin-induced cardiotoxicity

Mitochondria isolated from various sources exert similar cardioprotective effects

Mitochondrial transplantation activates glutamine metabolism in doxorubicin-treated heart

Sun et al., iScience 26, 107790
October 20, 2023
https://doi.org/10.1016/j.isci.2023.107790

iScience

CellPress
OPEN ACCESS

Article

Mitochondrial transplantation ameliorates doxorubicin-induced cardiac dysfunction via activating glutamine metabolism

Xiaolei Sun,[1,2,3,4] Hang Chen,[1,2,3,4,7] Rifeng Gao,[6] Ya Huang,[1,2,3,4] Yanan Qu,[1,2,3,4] Heng Yang,[8] Xiang Wei,[6] Shiyu Hu,[1,2,3,4] Jian Zhang,[1,2,3,4] Peng Wang,[1,2,3,4] Yunzeng Zou,[1,2,3,4,5] Kai Hu,[1,2,3,4] Junbo Ge,[1,2,3,4,5] and Aijun Sun[1,2,3,4,5,9,*]

SUMMARY

Doxorubicin is a wildly used effective anticancer agent. However, doxorubicin use is also related to cardiotoxic side effect in some patients. Mitochondrial damage has been shown to be one of the pathogeneses of doxorubicin-induced myocardial injury. In this study, we demonstrated that mitochondrial transplantation could inhibit doxorubicin-induced cardiotoxicity by directly supplying functional mitochondria. Mitochondrial transplantation improved contractile function and respiratory capacity, reduced cellular apoptosis and oxidative stress in cardiomyocytes. Mitochondria isolated from various sources, including mouse hearts, mouse and human arterial blood, and human induced pluripotent stem cell-derived cardiomyocytes (hiPSC-CMs), all exerted similar cardioprotective effects. Mechanically, mitochondrial transplantation activates glutamine metabolism in doxorubicin-treated mice heart and blocking glutamine metabolism attenuated the cardioprotective effects of mitochondrial transplantation. Overall, our study demonstrates that mitochondria isolated from arterial blood could be used for mitochondrial transplantation, which might serve as a feasible promising therapeutic option for patients with doxorubicin-induced cardiotoxicity.

INTRODUCTION

Doxorubicin is an anthracycline antibiotic, one of the most effective chemotherapeutic drugs for treating several types of cancer, including leukemias, lymphomas, and solid tumors. It inhibits cancer progression by interfering with DNA replication and transcription.[1,2] Despite the well-established anticancer efficacy, doxorubicin use is associated with several significant side effects including cardiomyopathy.[3] The incidence of electrophysiological abnormalities may be as high as 60% in patients after the first course of doxorubicin treatment.[4] Doxorubicin-induced cardiotoxicity is macroscopically characterized by cardiac enlargement, and biventricular dysfunction.[5,6] Impairing mitochondrial function is known to an important therapeutic mechanism of doxorubicin therapy, which might also be the crucial pathogenesis of doxorubicin-induced cardiotoxic side effect.[7] Previous studies showed that doxorubicin directly inhibits oxidative phosphorylation (OXPHOS) and increases oxidative stress in mitochondria,[8,9] whereas, doxorubicin-induced iron overload could further result in mitochondrial damaging.[10] It was reported that doxorubicin could promote cardiotoxicity by activating the opening of the mitochondrial permeability transition pores (mPTPs),[11] leading to cardiomyocytes death. The inhibitory effect of doxorubicin on nuclear topoisomerase 2β might also initiate a cardiotoxic cascade, ultimately lead to mitochondrial dysfunction and defective mitochondrial biogenesis due to nuclear damage.[12] The mitochondrial damage induced by doxorubicin has also been shown to trigger autophagic and mitophagic responses[13] as well as the mitochondria-dependent apoptotic pathway.[14,15] In view of the aforementioned evidence showing the therapeutic effects in terms of cancer therapy and deleterious effects in terms of cardiac toxicity of doxorubicin-induced mitochondrial dysfunction, it is reasonable to speculate that preserving or enhancing mitochondrial function may be a potential therapeutic approach to prevent/attenuate doxorubicin-induced cardiomyopathy.

[1]Department of Cardiology, Zhongshan Hospital, Fudan University, Shanghai 200032, P.R. China
[2]Shanghai Institute of Cardiovascular Diseases, Shanghai 200032, P.R. China
[3]NHC Key Laboratory of Viral Heart Diseases, Shanghai 200032, P.R. China
[4]Key Laboratory of Viral Heart Diseases, Chinese Academy of Medical Sciences, Shanghai 200032, P.R. China
[5]Institute of Biomedical Science, Fudan University, Shanghai 200032, P.R. China
[6]Shanghai Fifth People's Hospital, Fudan University, Shanghai 200240, P.R. China
[7]Cardiac Regeneration and Ageing Lab, Institute of Cardiovascular Sciences, Shanghai Engineering Research Center of Organ Repair, School of Life Science, Shanghai University, Shanghai 200444, P.R. China
[8]The Second Affiliated Hospital of Nanchang University, Nanchang 330000, P.R. China
[9]Lead contact
*Correspondence: sun.aijun@zs-hospital.sh.cn
https://doi.org/10.1016/j.isci.2023.107790

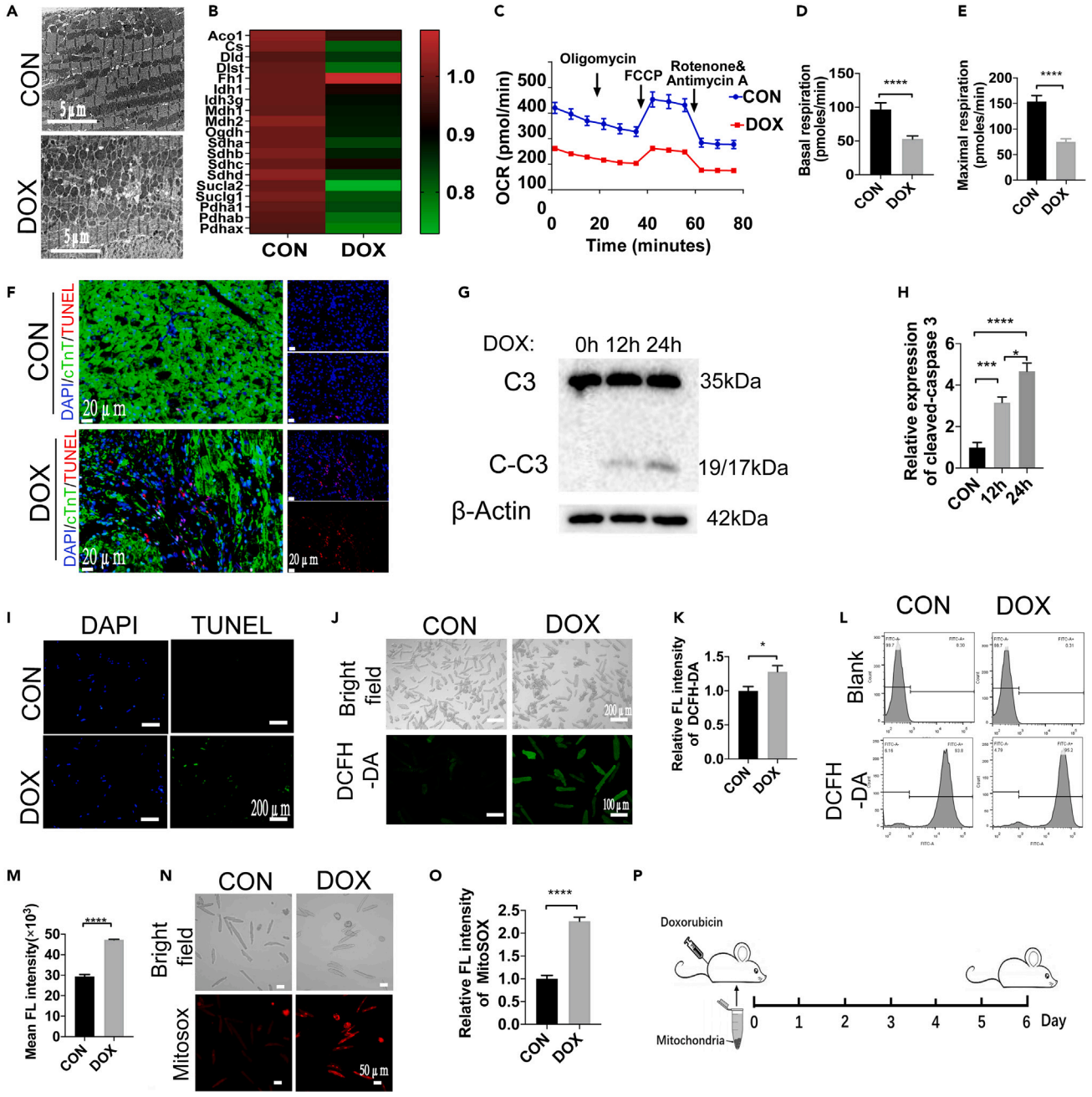

Figure 1. Doxorubicin (DOX) treatment causes mitochondrial dysfunction in cardiomyocytes

(A) Mouse hearts were analyzed by transmission electron microscopy 6 days after the administration of saline (upper) or DOX (15 mg/kg; lower). Scale bars, 5 μm.

(B) DOX inhibited the mRNA expression of genes associated with oxidative phosphorylation in the mouse heart. Control (CON, n = 4), DOX treatment (DOX, n = 4).

(C) DOX treatment decreased the oxygen consumption rate (OCR) in cardiomyocytes.

(D) Statistical analysis of basic OCR.

(E) Statistical analysis of maximal OCR.

(F) Apoptotic cardiomyocytes (red) were visualized by TUNEL assay in mouse hearts after the administration of saline (upper) or DOX (15 mg/kg; lower). Cell nuclei were stained with DAPI (blue). Cardiomyocytes were stained with cTnT (Green). Scale bars, 20 μm.

(G) Caspase-3 and cleaved-caspase-3 protein expression was detected in cultured cardiomyocytes after 0 h, 12 h, and 24 h of DOX treatment.

(H) Statistical analysis of cleaved caspase-3 protein expression.

(I) Cardiomyocyte apoptosis (green) was visualized by fluorescence microscopy in control and DOX-treated cardiomyocytes. Cell nuclei were stained with DAPI (blue). Scale bars, 200 μm.

Figure 1. *Continued*

(J) Cellular shape was analyzed by bright field microscopy and ROS levels were analyzed using DCFH-DA probes in both control and DOX-treated cardiomyocytes. Scale bars, 200 μm (bright field); 100 μm (DCFH-DA).

(K) Statistical analysis of DCFH-DA fluorescence intensity.

(L) Flow cytometer analysis of cellular ROS levels after DCFH-DA staining.

(M) Mean DCFH-DA fluorescence intensity of control and DOX-treated cells.

(N) Cellular shape was analyzed by bright field microscopy and mitochondrial ROS levels were analyzed by using MitoSOX probes in both control and DOX-treated cardiomyocytes. Scale bars, 50 μm (bright field).

(O) Relative MitoSOX fluorescence intensity of control and DOX-treated cells.

(P) Schematic diagram of the experimental protocol. All results are presented as the mean ± SEM. One-way ANOVA analysis followed by Tukey's post hoc test was applied for comparisons among multiple groups. Unpaired Student's t tests were used for comparisons between two groups. *$p < 0.05$, ***$p < 0.001$, ****$p < 0.0001$.

Mitochondrial transplantation is an innovative therapeutic strategy for the treatment of chronic diseases associated with mitochondrial dysfunction. Transplantation of platelet-derived mitochondria could ameliorate cognitive impairment and mitochondrial dysfunction in diabetic mice.[16] The transplantation of isolated mitochondria has been demonstrated to mitigate ischemia-reperfusion injury in the liver,[17] attenuate acute limb ischemia,[18] and enhance murine lung viability and recovery after ischemia-reperfusion injury.[19] Additionally, the transplantation of viable, respiratory-competent mitochondria has been shown to ameliorate mitochondrial damage within ischemic myocardial tissue.[20–23] Moreover, a series of studies by McCully et al.[24,25] have validated that autologous injection of mitochondria into the ischemic myocardial tissues of patients significantly ameliorated ischemia-reperfusion injury and cardiac dysfunction. Our previous study revealed that mitochondrial modification by acetaldehyde dehydrogenase 2 (ALDH2) could enhance the cardioprotective effects of mitochondrial transplantation after myocardial ischemia-reperfusion injury.[26] However, the effects of mitochondrial transplantation on doxorubicin-induced cardiotoxicity remain unexplored.

In this study, we verified that mitochondrial integrity served as a key determinant of doxorubicin-induced cardiotoxicity. We demonstrated that doxorubicin-induced mitochondrial dysfunction could activate apoptotic signaling and contribute to mitochondrial metabolic disorders in cardiomyocytes. We further showed that mitochondrial transplantation could effectively ameliorate these deleterious effects by enhancing mitochondrial dynamics and respiration as well as by reducing the production of reactive oxygen species (ROS). Additionally, we revealed similar cardioprotective effects after transplantation with mitochondria isolated from various sources, and illustrated that the activation of glutamine metabolism post mitochondrial transplantation contributed to the working mechanism of mitochondria transplantation in doxorubicin-treated cardiomyocytes. Our results suggest that mitochondria isolated from human arterial blood might be an ideal source for transplantation, the translational implication of this finding warrants further validation in future clinical studies.

RESULTS

Doxorubicin induces mitochondrial injury in cardiomyocytes

To determine mitochondrial changes induced by doxorubicin, we used transmission electron microscopy to observe the structure of mitochondria in the hearts of mice after the administration of doxorubicin (15 mg/kg) one dose for 6 days. As expected, doxorubicin induced morphological alterations in the mitochondria. Specifically, doxorubicin treatment caused mitochondrial disorganization and fragmentation in cardiomyocytes compared with the untreated controls. Vacuolization was also observed in mitochondria after doxorubicin treatment (Figure 1A). Accordingly, the mRNA expression of genes of mitochondrial OXPHOS pathways was significantly downregulated in cardiomyocytes after doxorubicin treatment (Figure 1B). Furthermore, a significantly reduced basic and maximal oxygen consumption rate (OCR) was observed in these cardiomyocytes, indicating impaired OXPHOS (Figures 1C–1E). Next, we evaluated cardiomyocyte apoptosis and found the colocalization of TdT-mediated dUTP Nick-End Labeling (TUNEL) positive signals with cTnT positive cardiomyocytes. As expected, doxorubicin-induced mitochondrial dysfunction was related to significantly increased cardiomyocyte apoptosis, the apoptosis ratio was 8.43% (Figure 1F). *In vitro*, isolated mouse cardiomyocytes were treated with doxorubicin (2 μM) for different time points. Cellular apoptosis was assessed by detecting the protein expression of cleaved caspase-3. Doxorubicin activated caspase-3 signaling in a time-dependent manner, and resulted in increased cellular death (Figures 1G and 1H). These findings were further confirmed by TUNEL assay in doxorubicin-treated cardiomyocytes, evidenced by apoptosis ratio of 38.65% (Figure 1I). Next, 2′,7′-dichlorofluorescin diacetate (DCFH-DA) probes were used to evaluate ROS production in response to doxorubicin treatment. As expected, doxorubicin treatment significantly elevated levels of ROS in cardiomyocytes (Figures 1J and 1K). The significantly increased ROS was further confirmed by flow cytometer analysis (Figures 1L and 1M). To determine the mitochondrial ROS changes, the MitoSOX staining was performed in both normal and doxorubicin-induced cardiomyocytes. We found that doxorubicin treatment significantly activated the mitochondrial ROS production, which was displayed in Figures 1N and 1O. Altogether, these results indicated that doxorubicin induced mitochondrial dysfunction, elevated ROS levels and cardiomyocyte apoptosis. We then tested the hypothesis that exogenous mitochondrial transplantation might ameliorate the doxorubicin-induced mitochondrial injury and reduce cardiomyocyte death in mice (Figure 1P).

Mitochondrial transplantation ameliorates doxorubicin-induced cardiac remodeling

To determine the therapeutic effects of mitochondrial transplantation, mitochondria were isolated from the hearts of Cox4i1-GFP mice prior to doxorubicin treatment (Figure 2A). As shown, these mitochondria contained well-defined, lamellar mitochondrial cristae, as well as clear

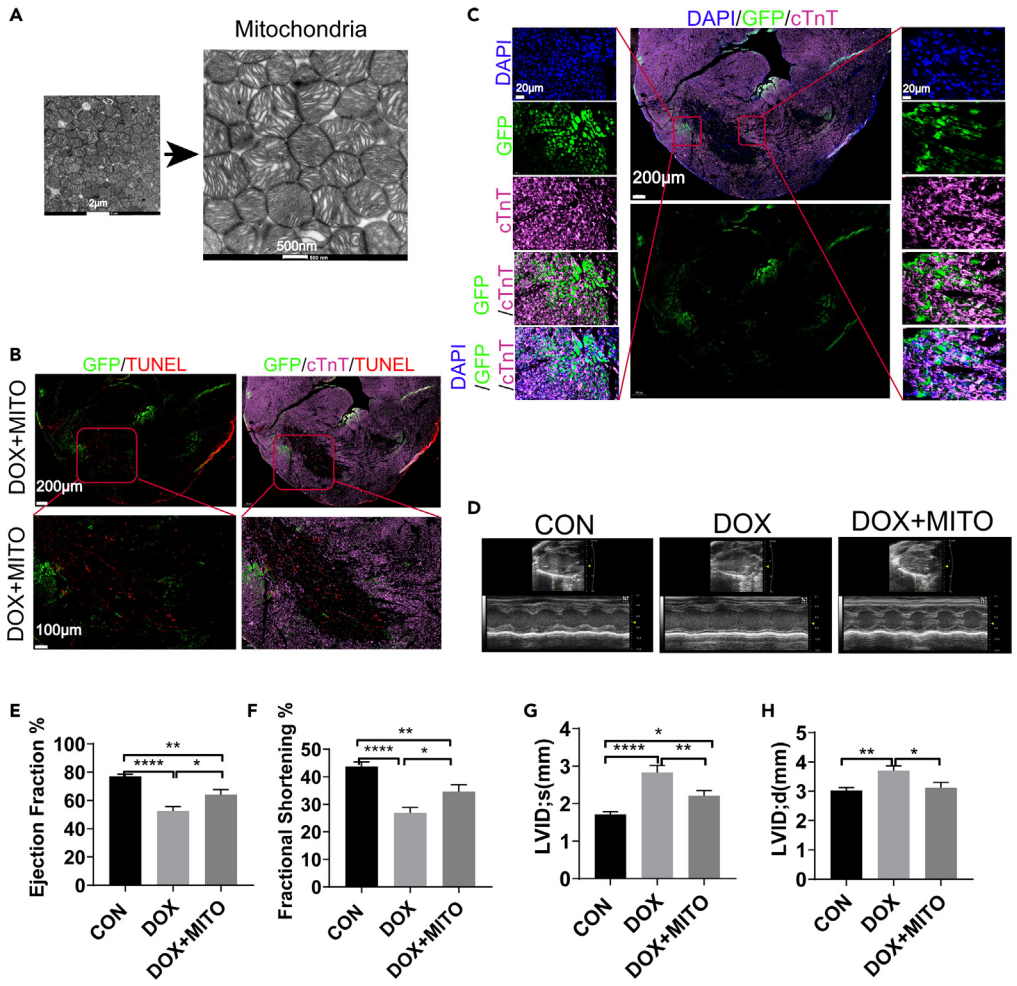

Figure 2. Mitochondrial transplantation enhances cardiac function after doxorubicin (DOX) treatment

(A) Mitochondrial integrity was confirmed by transmission electron microscopy. Scale bars, 2 μm (left); 500 nm (rightr).

(B) Transplanted mitochondria (green) were visualized in the myocardial tissues after injection for 3days. Apoptotic cell (TUNEL+: red). Cardiomyocytes were stained with cTnT (Purple). Scale bars, 200 μm (upper); 100 μm (lower).

(C) Location of GFP mitochondria in cardiomyocytes (Purple). Nuclear was stained with DAPI (blue). Scale bars, 200 μm (upper); 100 μm (lower); 20 μm (left and right).

(D) Cardiac function was assessed by echocardiography.

(E) Ejection fractions.

(F) Fractional shortenings.

(G and H) The end-systolic and diastolic left ventricular (LV) internal dimensions were measured. Control (CON, n = 15), DOX treatment (DOX, 15 mg/kg, n = 11), DOX treatment/mitochondrial transplantation (DOX+MITO, 15 mg/kg DOX, n = 11). All results are presented as the mean ± SEM. Statistical analysis was carried out by a one-way ANOVA analysis followed by Tukey's test for post hoc analysis. *$p < 0.05$, **$p < 0.01$, ****$p < 0.0001$. See also Figures S1–S3.

mitochondrial outer membrane. These mitochondria (total 50–100 μL of 1×10^5 mitochondria)[26] were then locally injected into the left ventricle of doxorubicin-treated mice heart. The transplanted mitochondria were visualized in the myocardial tissues (Figures 2B and 2C). The fluorescence staining showed that most of GFP mitochondria were located in the cardiomyocytes with positive cTnT fluorescence. It was calculated that the transplanted mitochondria account for 2.6% of the left ventricle. Next, cardiac function was assessed by echocardiography at day 6 (Figure 2D). Doxorubicin treatment substantially reduced the left ventricular ejection fraction (LVEF) and left ventricular fractional shortening (LVFS) parameters in mice (Figures 2E and 2F). As expected, cardiac function was improved by mitochondrial transplantation in this model. Specifically, the overall LVEF (68.90% vs. 48.69%) and LVFS (37.74% vs. 24.26%) were significantly increased in mice treated with mitochondrial transplantations compared to mice without mitochondrial transplantations. The doxorubicin-induced increased end-systolic (LVIDs) and diastolic (LVIDd) left ventricular internal dimensions could be significantly reversed by mitochondrial transplantation (Figures 2G and 2H). This cardioprotective role of mitochondrial transplantation in doxorubicin-induced cardiac injury was also determined in female mice (Figures S1A–S1C). Next, an EMT6 breast carcinoma model was developed to evaluate the effect of mitochondrial transplantation on the anti-cancer role of doxorubicin. As shown in Figures S2A and S2B, significantly tumor inhibition effect was observed for mice treated with

doxorubicin or mitochondrial transplantation. This antitumor effect was observed with a reduction in tumor volume by 44.46% and 44.56% of that of saline respectively (Figure S2C).

In addition, to clarify the restrictive conditions of mitochondrial transplantation in the protection of mice heart, the transplantation of normal and dysfunctional mitochondria was performed on healthy mice heart. Specifically, the normal and dysfunctional mitochondria were isolated from healthy and doxorubicin-treated mice heart, respectively. Then cardiac function was detected by echocardiography at day 6. Unexpectedly, results showed that normal mitochondria transplantation resulted in the reduction of LVEF from 67.93% to 55.09%, and LVFS decreased from 37.58% to 28.80%. In addition, transplantation of dysfunctional mitochondria decreased the LVEF from 67.93% to 46.52%, and the LVFS from 37.58% to 23.02% (Figures S3A–S3C). The aforementioned results indicated that the mitochondrial transfer to normal heart was harmful and decreased the heart function, which was further aggravated by dysfunctional mitochondrial transplantation. Altogether, these data indicated the cardioprotective role of mitochondrial transplantation was only observed in the injured heart induced by doxorubicin treatment.

Mitochondrial transplantation improves doxorubicin-induced cardiomyocyte contractile dysfunction

Because doxorubicin treatment has been shown to cause cardiac atrophy, we examined the effects of doxorubicin treatment in the presence and absence of mitochondrial transplantation on cardiomyocyte size and mitochondrial quantity in isolated cardiomyocytes. Doxorubicin treatment markedly reduced cardiomyocyte size as well as the MitoTracker Red fluorescence density, which indicated a reduced number of functional mitochondria in the isolated cardiomyocytes. However, these effects were reversed by mitochondrial transplantation (Figures 3A–3C). To further understand the internalization process of transplanted mitochondria, the isolated mitochondria were labeled with MitoTracker Green and transplanted. The mitochondria of control and doxorubicin-treated cardiomyocytes were stained with MitoTracker Red. The mitochondrial internalization was evidenced by the colocalization of green and red florescence by confocal imaging (Figure 3D). Next, we evaluated the contractile response of the cardiomyocytes isolated from doxorubicin-treated mice with or without mitochondrial transplantation. Consistent with the changes observed in cardiomyocyte size, doxorubicin treatment decreased while mitochondrial transplantation increased the resting cell length of the cardiomyocytes (Figure 3E). Additionally, we found that doxorubicin treatment caused contractile dysfunction in the cardiomyocytes, which was reversed by mitochondrial transplantation. Specifically, doxorubicin treatment induced an overall decrease in the maximal velocity of shortening/relengthening ($\pm$dl/dt) and peak shortening (% cell lengthening) in the cardiomyocytes; however, these were increased after mitochondrial transplantation (Figures 3F–3H). Likewise, doxorubicin treatment caused an elevated time to peak shortening/relengthening (TPS-s) in the cardiomyocytes, which was decreased after mitochondrial transplantation (Figures 3I and 3J). Altogether, doxorubicin impaired the mechanical contractility of the cardiomyocytes; however, this effect was reversed by mitochondrial transplantation.

Mitochondrial transplantation inhibits doxorubicin-induced cardiomyocyte apoptosis

To demonstrate the direct effects of mitochondrial transplantation on doxorubicin-induced apoptotic signaling in cardiomyocytes, we analyzed apoptosis as well as mitochondrial internalization in isolated cardiomyocytes *in vitro*. MitoTracker Green was used to visualize the transplanted mitochondria, and their internalization by cardiomyocytes was analyzed over time (Figure 4A). The results indicated that the doxorubicin-induced cardiomyocyte apoptosis was inhibited by mitochondrial transplantation. The apoptosis inhibition effect occurred after mitochondrial internalization and around 6 h after mitochondria transplantation (Figures 4B and 4C). Accordingly, significantly elevated levels of both 19-kD and 17-kD active caspase-3 were detected in the hearts of doxorubicin-treated mice that did not receive mitochondrial transplantations. However, mitochondrial transplantation inhibited caspase-3 activation (Figures 4D–4F). BAX is a member of the BCL-2 family, and its activation in the mitochondrial outer membrane is involved in the intrinsic pathway of apoptosis. BCL-2 is an anti-apoptotic or pro-survival protein. Next, we assessed the protein expression ratio of proapoptotic BAX and anti-apoptotic BCL-2 to evaluate the susceptibility of the cardiomyocytes to apoptosis. We found that the BAX/BCL-2 ratio was reduced in the hearts of the doxorubicin-treated mice that received mitochondrial transplantations compared with those that did not (Figures 4G and 4H). Additionally, TUNEL assay further confirmed that mitochondrial transplantation decreased apoptosis in the hearts of these mice (Figures 4I and 4J). These findings demonstrated that the cardio-protection exerted by mitochondrial transplantation may be due to anti-apoptotic effects in cardiomyocytes.

Mitochondrial transplantation reduces doxorubicin-induced oxidative stress in cardiomyocytes

Doxorubicin treatment causes a cardiotoxic cascade that can both directly and indirectly promote ROS production.[7] We used dihydroethidium (DHE) staining to evaluate the total ROS production after doxorubicin treatment in cardiomyocytes with or without subsequent mitochondrial transplantation. Doxorubicin treatment resulted in overtly elevated levels of ROS in the cardiomyocytes. However, these levels were significantly decreased after mitochondrial transplantation (Figures 5A and 5B). The redox cycling of doxorubicin primarily occurs in complex I of the mitochondrial respiration chain, making it the primary site for the generation of superoxide and other ROS.[8,27] Next, we analyzed mitochondrial ROS production using MitoSOX Red. Consistent with our other findings, doxorubicin-induced mitochondrial ROS production was significantly reduced after mitochondrial transplantation in the cardiomyocytes (Figures 5C and 5D) Manganese superoxide dismutase (MnSOD or SOD2) is a mitochondrial detoxification enzyme that catalyzes the conversion of superoxide to hydrogen peroxide.[28–30] The increased levels of mitochondrial ROS were further verified by the downregulation of MnSOD/SOD2 in the myocardial tissues of the doxorubicin-treated mice. However, mitochondrial transplantation resulted in the upregulation of MnSOD/SOD2 levels (Figures 5E and 5F). We next evaluated the levels of phosphorylated ataxia telangiectasia mutated (p-ATM) as a surrogate marker of DNA damage due to

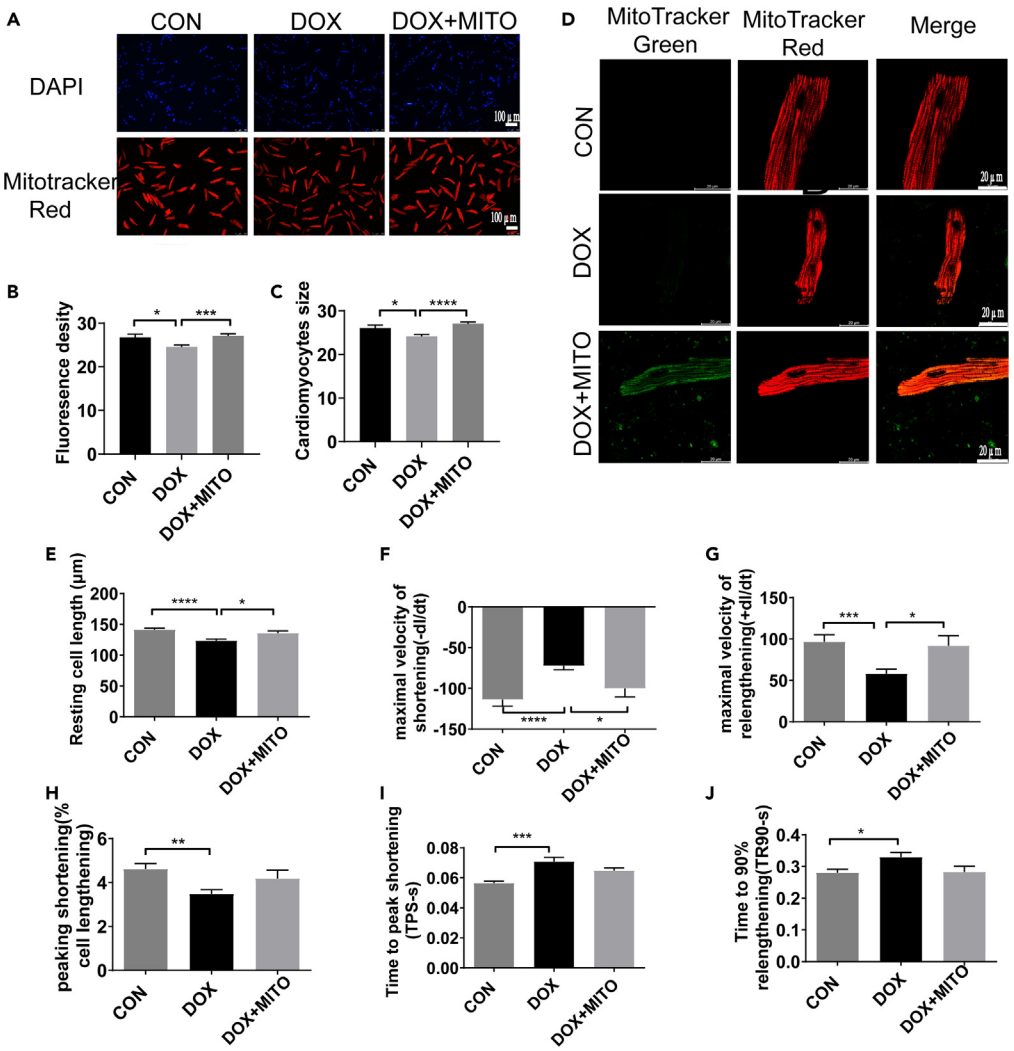

Figure 3. Mitochondrial transplantation enhances the mechanical function of cardiomyocytes after doxorubicin (DOX) treatment

(A) Mitochondria (red) were quantified by MitoTracker Red and fluorescence microscopy in cardiomyocytes isolated from mice. Control (CON, left), DOX treatment (DOX, middle), and DOX treatment/mitochondrial transplantation (DOX+MITO, right). Cell nuclei were stained by DAPI (blue). Scale bars, 100 μm.

(B) The MitoTracker Red fluorescence density was analyzed in the CON, DOX, and DOX+MITO mice.

(C) Mean cardiomyocyte size was calculated for the cardiomyocytes isolated from the CON, DOX, and DOX+MITO mice from panel A.

(D) Representative images of mitochondrial internalization into doxorubicin-induced cardiomyocyte.

(E–J) Contractile response of the cardiomyocytes. (E) Resting cell length, (F) maximal velocity of shortening (-dl/dt), (G) maximal velocity of relengthening (+dl/dt), (H) peak shortening (% cell lengthening), (I) time to peak shortening (TPS-s), and (J) time to 90% relengthening (TR90-s) were also calculated for the isolated cardiomyocytes. All results are presented as the mean ± SEM. Statistical analysis was carried out by a one-way ANOVA analysis followed by Tukey's test for post hoc analysis. *$p < 0.05$, ***$p < 0.001$, ****$p < 0.0001$.

the excessive amounts of ROS. Immunohistochemistry revealed a significant decrease in p-ATM levels in doxorubicin-treated cardiomyocytes after mitochondrial transplantation (Figures 5G and 5H). ROS-induced DNA damage is repaired via the damage-specific binding and catalytic activity of 8-oxoguanine DNA glycosylase (OGG1). However, its catalytic function can be inhibited by elevated levels of intracellular ROS.[31] As expected, OGG1 protein expression was downregulated in the doxorubicin-treated cardiomyocytes; however, mitochondrial transplantation reversed this (Figures 5I and 5J). These aforementioned data indicated the negative regulation between p-ATM and OGG1 in doxorubicin-treated mice heart. Next, to determine the specific regulation-ship between p-ATM and OGG1 post doxorubicin treatment, the OGG1 was overexpressed and knocked down with plasmid and siRNA transfection respectively. As expected, the data indicated that doxorubicin induced significant increase of p-ATM, which was further enhanced by OGG1 knock down, but significantly inhibited by OGG1 overexpression (Figures S4A and S4B). These results demonstrated the negative regulating relationship between p-ATM and OGG1 in doxorubicin-treated heart.

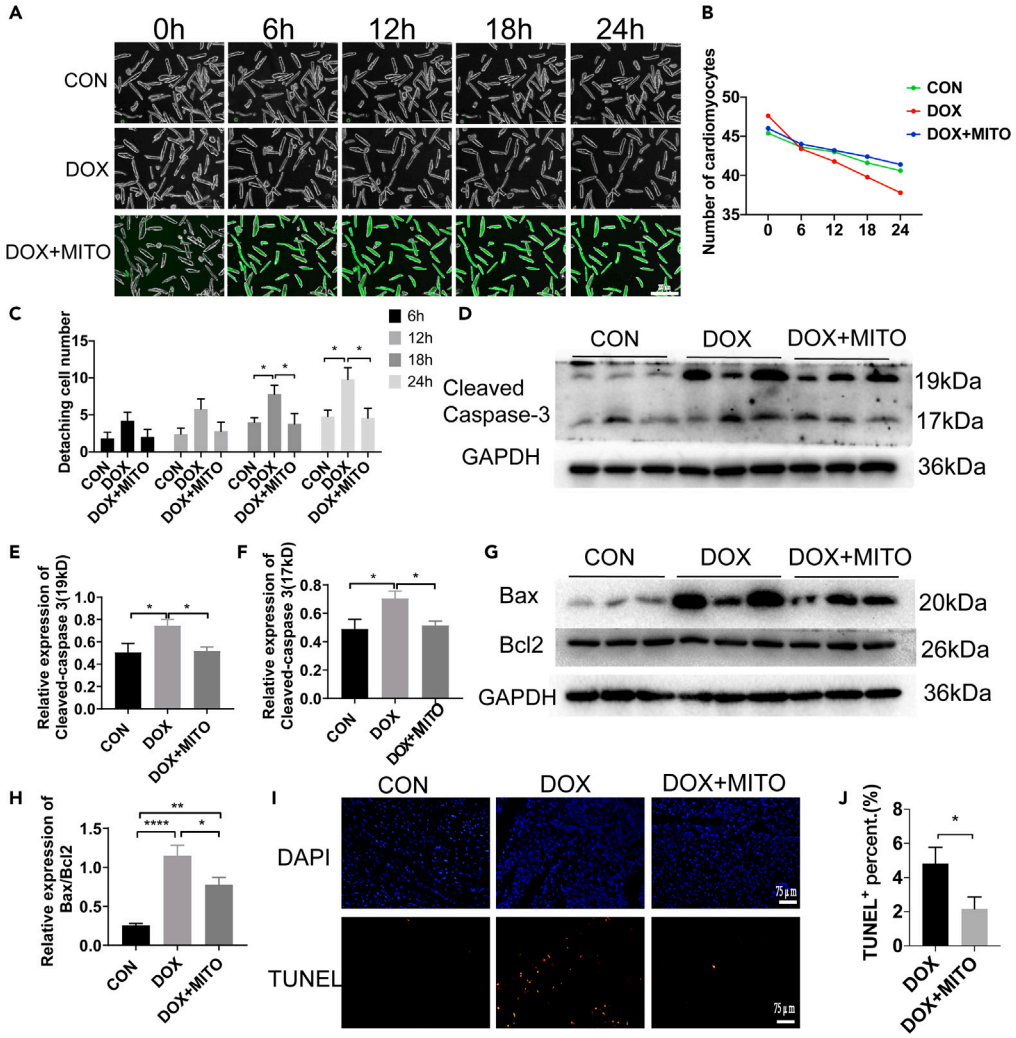

Figure 4. Mitochondrial transplantation protects against doxorubicin (DOX)-induced cardiac injury by inhibiting cardiomyocyte apoptosis

(A) Isolated cardiomyocytes were treated with DOX and incubated with or without mitochondria. Transplanted mitochondria were visualized by MitoTracker Green. Scale bar, 200 μm.

(B) Cardiomyocyte death was analyzed at different time points after DOX treatment or mitochondrial transplantation.

(C) Statistical analysis of detaching cell number after DOX treatment or mitochondrial transplantation.

(D) Cleaved caspase-3 levels were analyzed by Western blot in mice heart. Control (CON, left), DOX treatment (DOX, middle), and DOX treatment/mitochondrial transplantation (DOX+MITO, right).

(E and F) The statistic assay of relative protein expression levels of 19-kDa (E) and 17-kDa (F) cleaved caspase-3.

(G and H) The ratios of pro-apoptotic BAX and anti-apoptotic BCL-2 were measured by Western blot (G) and (H) calculated.

(I and J) Apoptotic cardiomyocytes (orange) were quantified by TUNEL assay after DOX treatment and mitochondrial transplantation. Cell nuclei were stained by DAPI (blue). Scale bars, 75 μm (n ≥ 3 per group). Control (CON), DOX treatment (DOX), and DOX treatment/mitochondrial transplantation (DOX+MITO). All results are presented as the mean ± SEM. One-way ANOVA analysis followed by Tukey's post hoc test was applied for comparisons among multiple groups. Unpaired Student's t tests were used for comparisons between two groups. *p < 0.05, **p < 0.01, ****p < 0.0001.

Mitochondrial transplantation ameliorates doxorubicin-induced mitochondrial dysfunction

We next analyzed key enzymes of the tricarboxylic acid (TCA) cycle, citrate synthase (CS), and isocitrate dehydrogenase 2 (IDH2), to evaluate mitochondrial ATP production after doxorubicin treatment and mitochondrial transplantation. The protein expression levels of CS and IDH2 were significantly downregulated after doxorubicin treatment, but they were restored by mitochondrial transplantation (Figures 6A–6C). To examine the effects of mitochondrial transplantation on OXPHOS after doxorubicin treatment, we isolated mitochondria from the hearts of the mice to determine the expression of mitochondrial respiratory complex I and II subunit proteins (Figure 6D). As expected, the reparative effects of mitochondrial transplantation on doxorubicin-induced cardiotoxicity were demonstrated

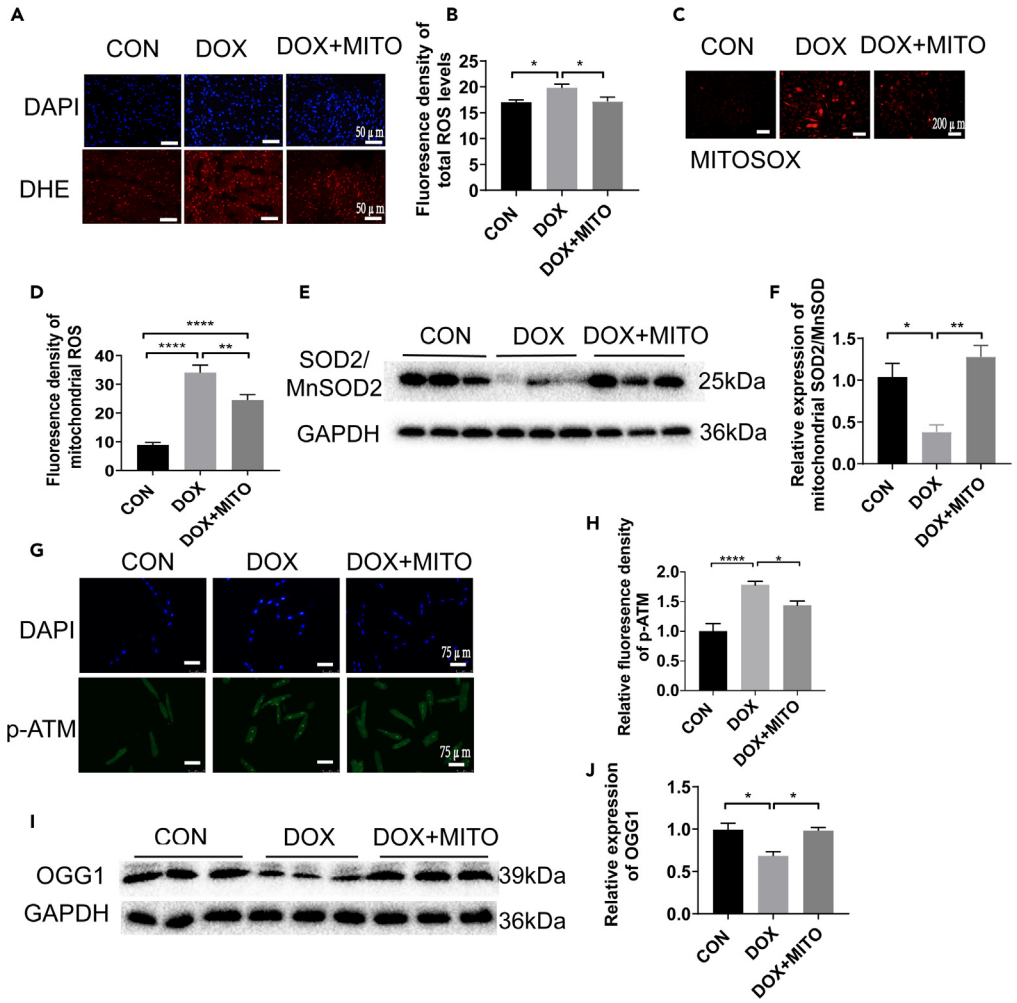

Figure 5. Mitochondrial transplantation inhibits doxorubicin (DOX)-induced oxidative stress in cardiomyocytes

(A) The effects of mitochondrial transplantation on DOX-induced ROS levels (red) were evaluated by dihydroethidium (DHE) staining in cardiomyocytes. Cell nuclei were stained by DAPI (blue). Scale bars, 50 μm (n ≥ 3 per group).

(B) The DHE fluorescence density was used as an indicator of ROS levels.

(C and D) MitoSOX staining was used to evaluate mitochondrial ROS production in mitochondria of cardiomyocytes.

(E and F) The protein expression levels of ROS scavenger manganese superoxide dismutase (MnSOD/SOD2) were evaluated by Western blot in mice heart.

(G and H) Immunostaining was used to evaluate the expression of phosphorylated ataxia-telangiectasia mutated (p-ATM, green) protein in cardiomyocytes. Cell nuclei were stained by DAPI (blue). Scale bars, 75 μm (n ≥ 3 per group).

(I and J) The protein expression levels of 8-oxoguanine DNA glycosylase (OGG1) were evaluated by Western blot in mice heart. Control (CON), DOX treatment (DOX), and DOX treatment/mitochondrial transplantation (DOX+MITO). All results are presented as the mean ± SEM. One-way ANOVA analysis followed by Tukey's post hoc test was applied for comparisons among multiple groups. *$p < 0.05$, **$p < 0.01$, ****$p < 0.0001$. See also Figure S4.

by the increased protein expression of mitochondrial complex I and II subunit proteins, including NADH:ubiquinone oxidoreductase subunit AB1 (NDUFAB1), succinate dehydrogenase (SDHD), and succinate dehydrogenase complex flavoprotein subunit A (SDHA) (Figures 6E and 6F). Next, the relative mRNA expression levels of NDUFAB1, SDHD, and SDHA were analyzed. The results indicated that doxorubicin treatment significantly inhibited the mRNA expression of NDUFAB1, SDHD, and SDHA, while this effect was not detected after mitochondrial transplantation (Figure 6G). Results indicated that the difference in the protein levels of NDUFAB1, SDHD, and SDHA might be the combined results of gene expression changes post mitochondria supplementation. We also assessed the mRNA expression of genes responsible for mitochondrial biogenesis and dynamics to further explore any alterations in mitochondrial function after doxorubicin treatment and mitochondrial transplantation. We found that doxorubicin treatment inhibited the mRNA expression of these genes, but their mRNA expression was reactivated after mitochondrial transplantation (Figures 6H and 6I). Degradation of dysfunctional mitochondria via mitophagy is a fundamental mechanism that regulates mitochondrial quality and quantity.

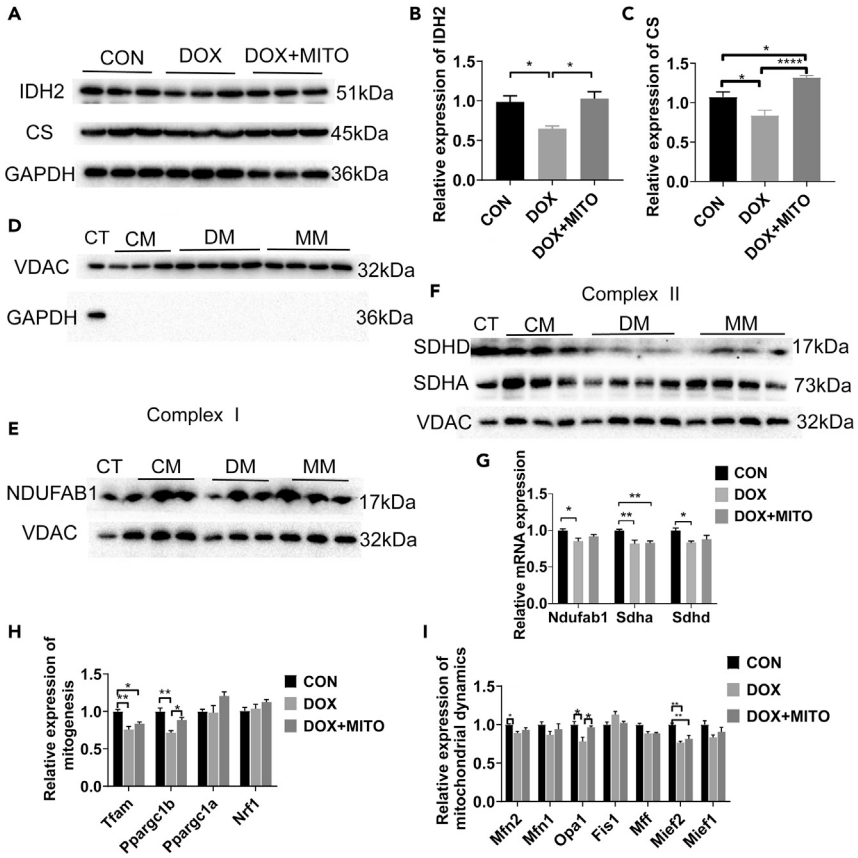

Figure 6. Mitochondrial transplantation improves doxorubicin (DOX)-induced mitochondrial dysfunction

(A–C) The protein expression levels of citrate synthase (CS) and isocitrate dehydrogenase 2 (IDH2) (A) were analyzed and quantified (B and C) by Western blot in mice heart after DOX treatment and mitochondrial transplantation.

(D) Mitochondrial purity was confirmed by Western blot. Mitochondria were represented by VDAC and the cytoplasm was represented by GAPDH. CM: mitochondria isolated from heart of control (CON). DM: mitochondria isolated from heart of DOX treatment (DOX). MM: mitochondria isolated from heart of DOX treatment/mitochondrial transplantation (DOX+MITO).

(E) The protein expression levels of NADH:ubiquinone oxidoreductase subunit AB1 (NDUFAB1) were analyzed by Western blot in mitochondria isolated from mouse hearts.

(F) The protein expression levels of succinate dehydrogenase (SDHD) and succinate dehydrogenase complex flavoprotein subunit A (SDHA) were analyzed by Western blot in mitochondria isolated from mouse hearts. CT, total protein; CM, control mitochondria; DM, DOX-treated mitochondria; MM, mitochondrial transplantation.

(G) Relative mRNA expression levels of NDUFAB1, SDHD, and SDHA.

(H) The relative mRNA expression of genes responsible for mitochondrial biogenesis, including transcription factor A, mitochondrial (*Tfam*), peroxisome proliferator-activated receptor gamma coactivator 1-alpha (*Ppargc1a*), peroxisome proliferator-activated receptor gamma coactivator 1-beta (*Ppargc1b*), and nuclear respiratory factor 1 (*Nrf1*) were analyzed.

(I) The relative mRNA expression of genes responsible for mitochondrial dynamics, including those that encode mitochondrial fusion (mitofusin 1 [*Mfn1*], mitofusin 2 [*Mfn2*], and optic atrophy 1 [*Opa1*]) and fission proteins (fission 1 [*Fis1*], mitochondrial fission factor [*Mff*], mitochondrial elongation factor 1 [*Mief1*], and mitochondrial elongation factor 2 [*Mief2*]) were analyzed. Control (CON), DOX treatment (DOX), and DOX treatment/mitochondrial transplantation (DOX+MITO). All results are presented as the mean ± SEM. One-way ANOVA analysis followed by Tukey's post hoc test was applied for comparisons among multiple groups. *$p < 0.05$, ***$p < 0.001$, ****$p < 0.0001$. See also Figure S5.

Accumulation of PINK1 on the outer membrane of mitochondria, resulting in Parkin translocation to mitochondria, constitutes key regulating factors of mitophagy. To evaluate the effect of mitochondrial transplantation on the fate of damaged mitochondria, the key regulating factors of mitophagy, PINK1, and Parkin, were detected in the hearts of the doxorubicin-treated mice. Compared with doxorubicin-treated heart, significantly upregulated protein expression of PINK1 and Parkin were observed in doxorubicin-treated heart with mitochondrial transplantation (Figures S5A–S5C), indicating that the cardioprotective role of mitochondrial transplantation was partially mediated by enhanced mitophagy. Altogether, these results demonstrated that mitochondrial transplantation significantly improved mitochondrial dysfunction induced by doxorubicin treatment.

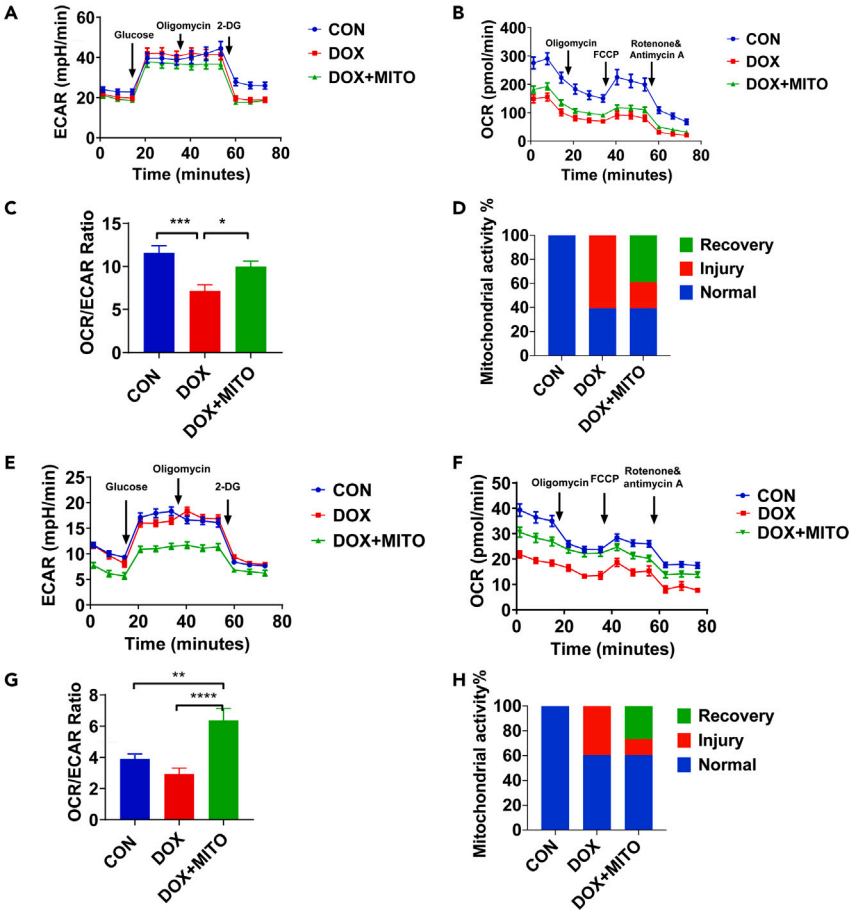

Figure 7. Mitochondrial transplantation improves metabolic function in cardiomyocytes after doxorubicin (DOX) treatment

(A) Extracellular acidification rates (ECARs) of cardiomyocytes isolated from control mice as well as DOX-treated mice with or without mitochondrial transplantation.

(B) Oxygen consumption rates (OCRs) of cardiomyocytes isolated from control mice as well as DOX-treated mice with or without mitochondrial transplantation.

(C) The calculated OCR/ECAR ratios to indicate mitochondrial respiratory capacity in the cardiomyocytes.

(D) The mitochondrial activity calculated in cardiomyocytes isolated from control mice as well as DOX-treated mice with or without mitochondrial transplantation.

(E) ECARs of control and doxorubicin-treated H9C2 cells with or without mitochondrial transplantation.

(F) OCRs of control and doxorubicin-treated H9C2 cells with or without mitochondrial transplantation.

(G) The calculated OCR/ECAR ratios to indicate mitochondrial respiratory capacity in the H9C2 cells.

(H) The mitochondrial activity calculated in control and doxorubicin-treated H9C2 cells with or without mitochondrial transplantation. All results are presented as the mean ± SEM. One-way ANOVA analysis followed by Tukey's post hoc test was applied for comparisons among multiple groups. *$p < 0.05$, **$p < 0.01$, ***$p < 0.001$, ****$p < 0.0001$.

Mitochondrial transplantation attenuates doxorubicin-induced cardiotoxicity by improving the respiratory capacity of cardiomyocytes

Next, we assessed the metabolic changes induced by doxorubicin treatment and mitochondrial transplantation in cardiomyocytes using a Seahorse XF96 Analyzer. The extracellular acidification rates (ECARs) and oxygen consumption rates (OCRs) were measured as indexes of glycolysis and OXPHOS, respectively, in cardiomyocytes isolated from control mice as well as doxorubicin-treated mice with or without mitochondrial transplantation. The OCR/ECAR ratio was used to indicate the mitochondrial respiratory capacity of the cardiomyocytes. This ratio was significantly reduced after doxorubicin treatment; however, it was preserved after mitochondrial transplantation (Figures 7A–7C). Given that mitochondrial respiration capacity could reflect mitochondrial function, we therefore used the basic respiration capacity as the quantitative parameter of healthy and damaged mitochondria after mitochondria transplantation. The percent of damaged mitochondria induced by doxorubicin treatment in primary cardiomyocytes accounted for 60.67%, among which 38.85% was recovered after mitochondrial transplantation (Figure 7D). These metabolic effects of mitochondrial transplantation were further confirmed *in vitro* using H9C2 rat myoblast cells (Figures 7E–7G). Consistent with our previous results, a reduced OCR/ECAR ratio was observed in the H9C2 cells after doxorubicin treatment,

but it was preserved with mitochondrial transplantation. Additionally, mitochondrial injury accounted for 39.66% in doxorubicin-induced H9C2, which was reduced to 13.08% after mitochondrial transplantation (Figure 7H).

Mitochondria isolated from various sources exert similar cardioprotective effects against doxorubicin-induced cardiotoxicity

To demonstrate the feasibility of mitochondrial transplantation for therapeutic use, we isolated mitochondria for transplantation from arterial blood and human induced pluripotent stem cell-derived cardiomyocytes (hiPSC-CMs) (Figure 8A). The reason for isolating mitochondria from arterial blood lies in the different metabolic substances presented in arterial and venous blood. To further verify the respiratory difference of mitochondria in arterial and venous blood, the membrane potential of mitochondria in arterial and venous blood was detected with TMRE staining. As expected, the TMRE fluorescence of mitochondria from arterial blood was significantly increased (up to 6 times) in comparison with that from venous blood (Figure S6A). The purity of the isolated mitochondria was confirmed by Western blot. TOM20 detection was used to represent the mitochondria, whereas GAPDH was used to represent the cytoplasm. Additionally, MitoTracker Green was used to directly image the isolated mitochondria. Viable mitochondria were successfully isolated from mouse arterial blood (Figures 8B and 8C), and their cardioprotective effects were observed in mice after doxorubicin treatment. Mitochondrial transplantation significantly improved the overall LVEF and LVFS (59.86% and 31.43% vs. 54.17% and 27.11%) in doxorubicin-treated mice (Figures 8D and 8E). Mitochondria were also successfully isolated from human arterial blood (Figures 8F and 8G). Transplantation with these mitochondria also significantly improved the overall LVEF and LVFS (70.52% and 39.21% vs. 59.57% and 31.05%) in doxorubicin-treated mice (Figures 8H and 8I). Consistently, similar changes in the overall LVEF and LVFS (53.76% and 27.50% vs. 47.55% and 23.59%) of doxorubicin-treated mice were observed after transplantation with mitochondria isolated from human iPSCs-CMs (Figures 8J and 8K). These results demonstrated the cardioprotective effects of transplantation with mitochondria isolated from various sources. However, we compared these effects to verify the optimal mitochondrial source. Our data demonstrated that transplantation with mitochondria isolated from mouse hearts (Figures 2D–2H) and human arterial blood improved cardiac function the most after doxorubicin treatment (Figures 8L and 8M), suggesting these as optimal mitochondrial sources. It is known that non-autologous therapies may cause an immune response. Therefore, the non-autologous immune response was evaluated in heart induced by doxorubicin treatment and human mitochondrial transplantation, the expression of neutrophils and monocytes marker was observed by flow cytometry. Results were showed as following, which revealed that the activation or infiltration of neutrophils and monocytes could not be affected by mitochondrial transplantation (Figures S7A–S7D).

Mitochondrial transplantation restores metabolic profile after doxorubicin-induced cardiotoxicity

We used liquid chromatography-tandem mass spectrometry (LC-MS/MS) to determine the metabolite profiles of the doxorubicin-treated hearts with or without mitochondrial transplantation. Then, we assessed the metabolome associated with the functional characteristics of mitochondrial transplantation in the doxorubicin-treated heart. A total of 8,794 valid peaks were ultimately identified and quantified. The differences in the metabolic physiology between the doxorubicin-treated hearts with or without mitochondrial transplantation were easily detected using the unsupervised principal component analysis (PCA) and orthogonal partial least squares discriminant analysis (OPLS-DA). The results indicated that the data distribution and the separation in were stable and reliable (Figure 9A). All of the parameters ($R2X = 0.632$, $R2Y = 0.914$, and $Q2 = 0.56$) considered for classification by the software were stable and accurate for prediction. The R2 and Q2 intercept values determined after 200 permutations were 0.94 and −0.16, respectively (Figure 9B). The negative Q2 intercept value indicated that the robustness of the models was valid and at low risk of overfitting. These data demonstrated that the comparison between the doxorubicin-treated heart (D) and the doxorubicin-treated heart with mitochondrial transplantation (M) was valid and that the OPLS-DA model could be used in subsequent analyses. Furthermore, a total of 469 metabolites were identified based on the following criteria: variable importance in the projection (VIP) values > 1.0 (calculated using the OPLS-DA model) and p values < 0.05 (calculated using the Student's *t* test). Between the D and M group, 392 metabolites were upregulated and 77 were downregulated (Figure 9C). A heatmap was created to visualize the differences in the major abundant metabolites between the D and M group (Figure 9D). We performed Kyoto Encyclopedia of Genes and Genomes (KEGG) pathway analysis to summarize the distribution of the metabolic pathways with the most significantly altered metabolites between the D and M group. The differentially abundant metabolites were identified based on both the -ln (p value) and pathway impact scores. The most relevant metabolic pathways were "D-glutamine and D-glutamate metabolism" (Figure 9E). Besides, in the comparison with D group, the significant increased glutamine was observed in M group (Figure 9F). These data suggested that D-glutamine and D-glutamate metabolism was activated in response to mitochondrial transplantation after doxorubicin-induced myocardial injury. Next, we analyzed the protein expression of glutaminase (GLS), the rate-limiting enzyme responsible for converting glutamine to glutamate,[32] in the hearts of the mice. As expected, GLS protein expression was significantly reduced in the doxorubicin-treated heart, but this was remarkably reversed by mitochondrial transplantation (Figures 9G and 9H). In addition, to illustrate the cardio-protection role of human-derived mitochondria in doxorubicin-induced cardiotoxicity model, we analyzed the protein expression of GLS in the hearts of the mice. Results demonstrated that GLS expression was significantly declined in the doxorubicin-treated heart, but this was remarkably reversed by human derived-mitochondrial transplantation (Figures S8A and S8B). Taken together, these results indicated that mitochondrial transplantation activated glutamine metabolism involving GLS.

To determine the role of glutamine metabolism induced by mitochondrial transplantation in doxorubicin-induced cardiomyocytes, the rate-limiting enzyme GLS, responsible for converting glutamine to glutamate, was silenced in H9C2 (Figure S9A). Then the protective role of mitochondrial transplantation was assessed by detecting the cellular apoptosis, ROS production, mitochondrial respiratory and

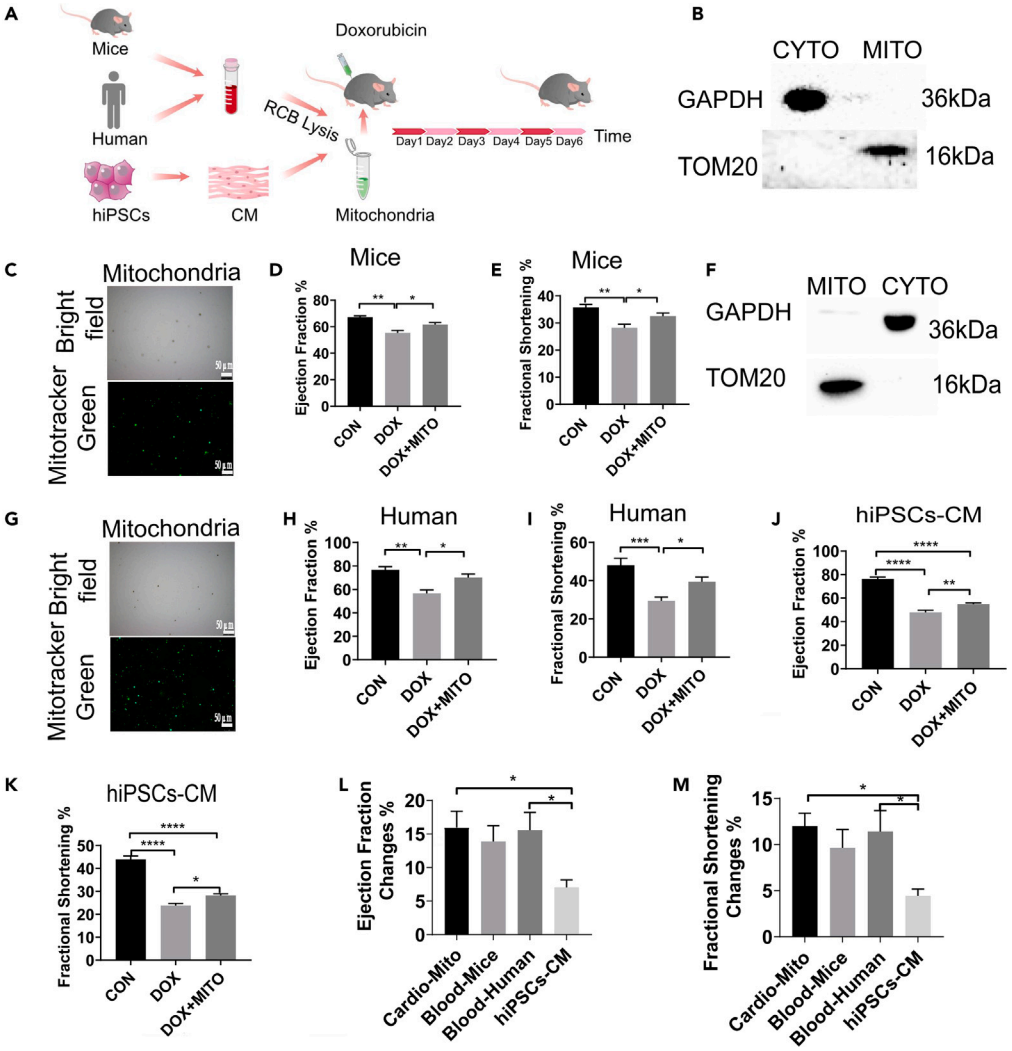

Figure 8. Mitochondria isolated from different sources exert similar cardioprotective effects

(A) Mitochondria were isolated from human and mouse arterial blood and human induced pluripotent stem cell-derived cardiomyocytes (hiPSC-CMs). RCB, red blood cell; CM, cardiomyocyte.

(B) The purity of the mitochondria isolated from mouse arterial blood was confirmed by Western blot. Mitochondria were represented by TOM20, and the cytoplasm was represented by GAPDH.

(C) The mitochondria isolated from mouse arterial blood were visualized using MitoTracker Green and fluorescence microscopy.

(D and E) The ejection fraction (D) and fractional shortening (E) parameters were measured in the mice after transplantation with mitochondria isolated from mouse arterial blood. Control (CON, n = 4), doxorubicin (DOX) treatment (DOX, n = 13), DOX treatment/mitochondrial transplantation (DOX+MITO, n = 13).

(F) The purity of the mitochondria isolated from human arterial blood was confirmed by Western blot. Mitochondria were represented by TOM20, and the cytoplasm was represented by GAPDH.

(G) The mitochondria isolated from human arterial blood were visualized using MitoTracker Green and fluorescence microscopy.

(H and I) The ejection fraction (H) and fractional shortening (I) parameters were measured in the mice after transplantation with mitochondria isolated from human arterial blood. CON (n = 5), DOX (n = 10), DOX+MITO (n = 10).

(J and K) The ejection fraction (J) and fractional shortening (K) parameters were measured in the mice after transplantation with mitochondria isolated from human iPSC-CMs. CON (n = 8), DOX (n = 9), DOX+MITO (n = 11).

(L and M) The ejection fraction (L) and fractional shortening (M) parameters were compared after transplantation with the mitochondria isolated from the different sources. Cardio-Mito (n = 9), Blood-Mice (n = 11), Blood-Human (n = 9), hiPSC-CMs (n = 11). All results are presented as the mean ± SEM. One-way ANOVA analysis followed by Tukey's post hoc test was applied for comparisons among multiple groups. *p < 0.05, **p < 0.01, ***p < 0.001, ****p < 0.0001. See also Figures S6 and S7.

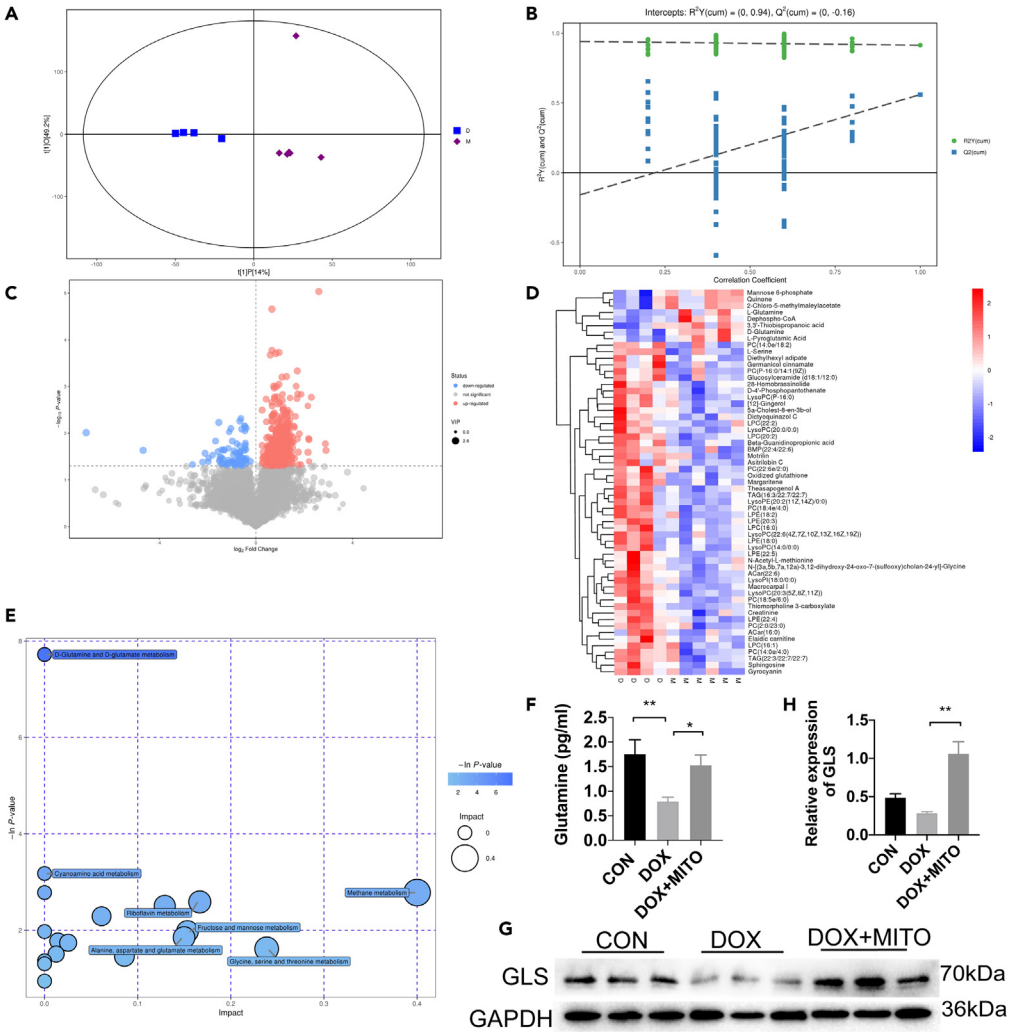

Figure 9. Glutamine and glutamate metabolic pathway activation in doxorubicin (DOX) treated heart after mitochondrial transplantation

(A and B) Derived PCA score plot, derived OPLS-DA score plots, and corresponding validation plots of OPLS-DA from the metabolite profiles of the DOX-induced heart (D groups) and mitochondria-exposed DOX heart (M groups).

(C) Volcano plot of the D and M groups, where each point represented a metabolite. Red dots represented upregulated metabolites, blue dots represented downregulated metabolites, and gray dots indicated nonsignificant differences.

(D) Heatmap of the significantly altered metabolites in the D and M groups. Individual samples (horizontal axis) and metabolites (vertical axis) were separated using hierarchical clustering. The color scale was noted in the upper right corner. The relative metabolite level was depicted according to color scale. Red indicated upregulation, and blue indicated downregulation.

(E) Bubble diagrams of the metabolic pathway topology analysis. The x axis represented pathway enrichment, and the y axis represented the pathway impact values.

(F) Glutamine (pg/ml) levels analysis in mice serum of the D and M groups.

(G) GLS levels were analyzed by Western blot in mice heart after DOX treatment or mitochondrial transplantation. Control (CON, left), DOX treatment (DOX, middle), and DOX treatment/mitochondrial transplantation (DOX+MITO, right).

(H) The statistic assay of relative protein expression levels of GLS. All results are presented as the mean ± SEM. One-way ANOVA analysis followed by Tukey's post hoc test was applied for comparisons among multiple groups. *$p < 0.05$, **$p < 0.01$. See also Figures S8 and S9.

mitochondrial membrane potential. Results indicated that the decreased protein expression of active caspase 3 induced by mitochondrial transplantation was re-activated by GLS knock down in doxorubicin-treated H9C2 (Figure S9B). Next, ROS production was evaluated by DCFH-DA probes staining in response to doxorubicin treatment. Compared with mitochondrial transplantation, elevated levels of ROS were detected in doxorubicin-treated H9C2 with GLS knock down (Figure S9C). Furthermore, a significantly reduced OCR was also observed in doxorubicin-treated H9C2 with GLS knock down, indicating that the restored OXPHOS induced by mitochondrial transplantation was impaired with GLS knock down (Figure S9D). To further determine the effect of GLS knock down on mitochondrial function recovery, mitochondrial membrane potential was detected by using TMRE staining. Compared with doxorubicin treatment, the significantly increased

mitochondrial membrane potential was observed in H9C2 with mitochondrial transplantation. However, this improvement of mitochondrial membrane potential was significantly inhibited after GLS knock down (Figure S9E).

Furthermore, additional experiments were performed to determine the relationship between the glutamine metabolism with original or supplementary mitochondrial activity. Specifically, we isolated mitochondria from both healthy mice heart and doxorubicin-induced mice heart, which represented healthy and dysfunctional mitochondria, respectively. Then the mitochondria were locally injected into the hearts of the mice after doxorubicin (15 mg/kg) treatment. Next, cardiac function was assessed by echocardiography at day 6 (Figure S9F). Results demonstrated that cardiac function was improved by healthy mitochondrial transplantation in doxorubicin-treated mice. Specifically, the overall LVEF (58.34% vs. 43.74%) and LVFS (30.68% vs. 21.34%) were significantly increased in mice treated with mitochondrial transplantations compared to mice without mitochondrial transplantations. However, the cardiac function was impaired after transplantation of dysfunctional mitochondria, evidenced by decreased LVEF from 58.34% to 45.37% and LVFS from 30.68% to 22.42% (Figures S9G and S9H). Moreover, compared with the healthy-mitochondrial transplantation, dysfunctional-mitochondrial transplantation significantly increased apoptosis levels in doxorubicin-induced mice heart, indicated with increased protein expression of cleaved-caspase 3. The GLS changes were detected to evaluate the effect of transplanted-mitochondrial activity on glutamine metabolism. Results demonstrated that healthy-mitochondrial transplantation upregulated GLS protein expression, while this upregulation was inhibited by dysfunctional-mitochondrial transplantation (Figure S9I). These findings demonstrated that the effect of mitochondrial transplantation is induced by the increased glutamine metabolism of the supplementation of new and undamaged mitochondria, rather than the original damaged mitochondria.

Inhibition of glutamine metabolism reverses the cardioprotective effects of mitochondrial transplantation against doxorubicin-induced cardiotoxicity

To verify the activation and protective effects of the glutamine metabolic pathway following mitochondrial transplantation in the doxorubicin-treated heart, glutamine antagonists, 6-diazo-5-oxo-*l*-norleucine (DON) and JHU083, were used for subsequent *in vitro* and *in vivo* experiments, respectively. Survival rate analysis revealed that mitochondrial transplantation resulted in an increased survival rate of 86.7% after doxorubicin treatment, whereas a survival rate of only 60% was observed without mitochondrial transplantation. However, inhibition of glutamine metabolism using JHU083 significantly reduced the survival rate to 65% after mitochondrial transplantation (Figure 10A). To further confirm the essential role of glutamine metabolism in the cardio-protection associated with mitochondrial transplantation, cardiac function was assessed by echocardiography (Figure 10B). Our previous results demonstrated that mitochondrial transplantation substantially improved the doxorubicin-induced reduction in the LVEF and LVFS parameters in mice; however, this cardioprotective effect was strongly attenuated by JHU083 treatment. This was shown by a significantly decreased overall LVEF (54.07% vs. 63.62%) and LVFS (27.46% vs. 34.09%) compared with doxorubicin-treated mice that received mitochondrial transplantations but not JHU083 treatment (Figures 10C and 10D). Furthermore, the glutamine antagonists JHU083 was also used in the doxorubicin-treated heart post human derived mitochondrial transplantation. Echocardiography was analyzed to illustrate the cardiac function (Figure S8C). The results of LVEF (Figure S8D) and LVFS (Figure S8E) showed that JHU083 treatment substantially reduced the human mitochondrial transplantation induced improvement in the LVEF and LVFS parameters in doxorubicin-treated mice heart. Compared with doxorubicin-treated mice that received human mitochondrial transplantations, a significantly decreased LVEF (52.69% vs. 60.18%) and LVFS (26.75% vs. 31.67%) was observed in the presence of JHU083. We next performed microscopic analysis of the cardiac tissues, and hematoxylin and eosin (H&E) staining revealed that doxorubicin treatment significantly decreased the cardiomyocyte cross-sectional area as well as the overall cardiac volume. These effects were reversed by mitochondrial transplantation; however, JHU083 treatment inhibited the cardioprotective effects of mitochondrial transplantation (Figure 10E). Next, we analyzed the ROS production resulting from doxorubicin treatment and thus promoting a cardiotoxic cascade. We used DHE staining to evaluate the ROS levels after doxorubicin and JHU083 treatment in the hearts of the mice with or without mitochondrial transplantation. Mitochondrial transplantation resulted in an overtly lower DHE fluorescence density compared with that in the hearts of doxorubicin-treated mice that did not receive mitochondrial transplantations. However, JHU083 treatment significantly increased this low DHE fluorescence density after mitochondrial transplantation (Figures 10F and 10G). Next, we analyzed mitochondrial ROS production *in vitro* using MitoSOX Red. Inhibition of glutamine metabolism using DON significantly increased ROS production, which was reduced after mitochondrial transplantation compared with doxorubicin-treated cardiomyocytes without mitochondrial transplantation (Figures 10H and 10I). These results demonstrated the essential role of glutamine metabolism induced by mitochondrial transplantation in the doxorubicin-treated heart.

Additionally, the glutamine supplementation was performed to further verify the cardio-protection of glutamine metabolism induced by mitochondrial transplantation in the doxorubicin-treated heart. Specifically, the doxorubicin (15 mg/kg) treated mice were further treated with or without 4% glutamine in the drinking water for 6 days. Next, cardiac function was assessed by echocardiography at day 6 (Figure S10A). Doxorubicin treatment substantially reduced the LVEF and LVFS in mice. Unexpectedly, cardiac function was not improved after glutamine supplementation (Figures S10B and S10C). Next, H&E staining was performed to microscopically analyze the cardiac tissues. Results revealed that doxorubicin treatment significantly decreased the overall cardiac volume and increased the left ventricular diameter. While these parameters could not be improved by glutamine supplementation (Figure S10D), these findings demonstrated that mitochondrial transplantation effectively ameliorated doxorubicin-induced cardiac remodeling by glutamine metabolism activation, which could not be replaced only with glutamine supplementation.

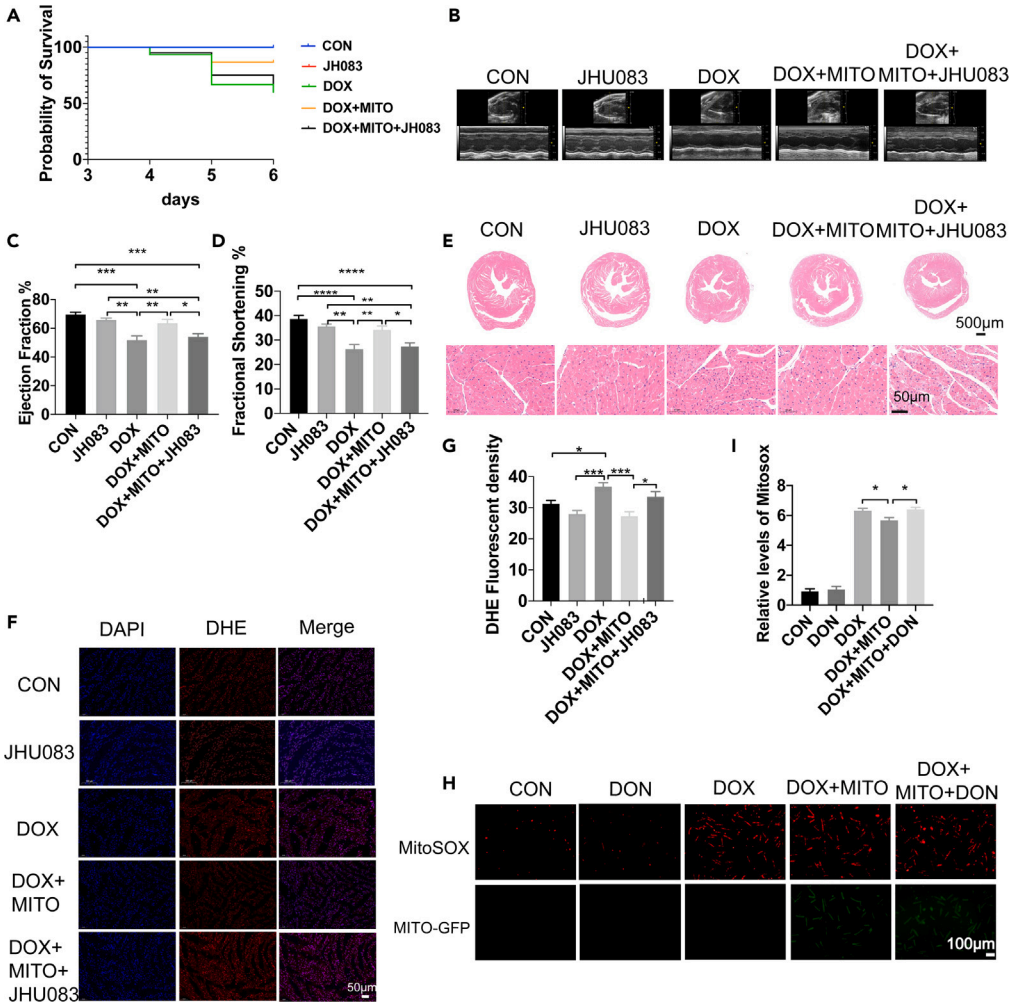

Figure 10. Glutamine metabolic inhibition compromises the cardioprotective role of mitochondrial transplantation after doxorubicin (DOX) treatment

(A) The survival rate was calculated after JHU083 treatment and mitochondrial transplantation in DOX treated mice.

(B) Cardiac function was assessed by echocardiography. Control (CON, n = 7), Control +JH083(JH083, n = 7), DOX treatment (DOX, 15 mg/kg, n = 8), DOX treatment/mitochondrial transplantation (DOX+MITO, 15 mg/kg DOX, n = 11), DOX treatment/JHU083 treatment/mitochondrial transplantation (DOX+MITO+JHU083, 15 mg/kg DOX, 1 mg/kg JHU083, n = 11).

(C) Ejection fractions.

(D) Fractional shortenings.

(E) Representative left ventricular (LV) cross-sections (after 6 days of DOX and JHU083 treatment or mitochondrial transplantation) stained with hematoxylin and eosin (H&E) stain dye. Scale bars, 50 μm (n ≥ 3 per group).

(F) The effects of mitochondrial transplantation on DOX-induced ROS levels (red) were evaluated by dihydroethidium (DHE) staining in cardiomyocytes. Cell nuclei were stained by DAPI (blue). Scale bars, 50 μm (n ≥ 3 per group).

(G) Statistical analysis of the DHE fluorescence density, used as an indicator of ROS levels.

(H) MitoSOX staining was used to evaluate mitochondrial ROS production in mitochondria of cardiomyocytes.

(I) Statistical analysis of the MitoSOX fluorescence density, Scale bars, 100 μm. All results are presented as the mean ± SEM. One-way ANOVA analysis followed by Tukey's post hoc test was applied for comparisons among multiple groups. *p < 0.05, **p < 0.01, ***p < 0.001, ****p < 0.0001. See also Figures S8 and S10.

Sustained myocardial protection of mitochondrial transplantation against doxorubicin-induced cardiotoxicity

The GFP mitochondria isolated from Cox4i1-GFP mice was tracked at different time points after single transplantation in mice heart. As shown in the following Figures S11A–S11D, the GFP fluorescence could be detected at 3 days and 1 week, gradually disappeared after transplantation at 2 weeks and at 3 weeks. Then the continuous contributions of mitochondrial transplantation against doxorubicin-induced cardiomyopathy were investigated in animals received long-term doxorubicin treatment (Figure 11A). Specifically, the mice received weekly intraperitoneally doxorubicin (5 mg/kg) doses for 4 weeks followed by 4 dose-free weeks. Dexrazoxane (DEX), the only drug approved by the FDA for preventing doxorubicin-induced cardiotoxicity in cancer patients, was used in our present study. For the DEX treatment, the mice received

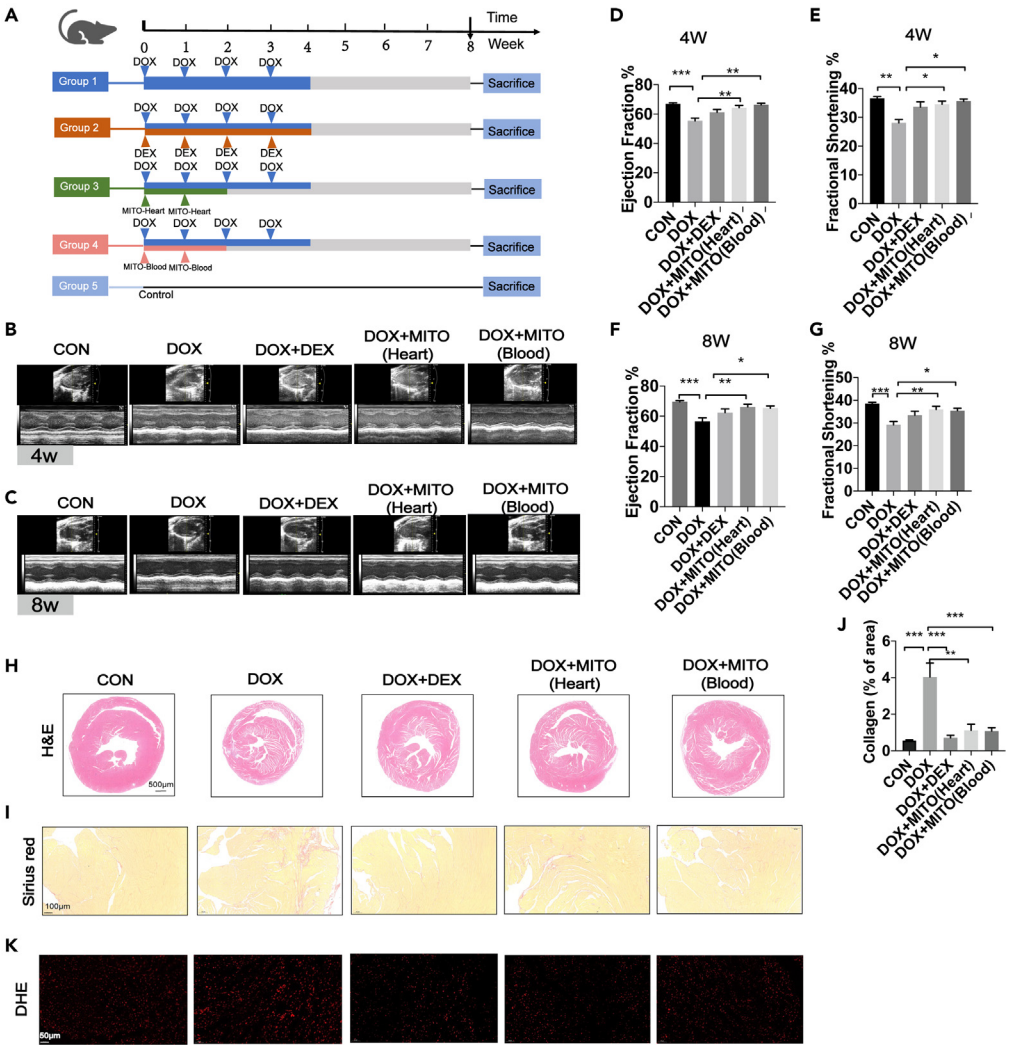

Figure 11. Long-term cardioprotective role of mitochondrial transplantation after doxorubicin (DOX) treatment

(A) Schematic diagram of the experimental protocol.

(B and C) Representative images of echocardiographic assay at 4 weeks (B) and 8 weeks (C). Control (CON, n = 8), DOX treatment (DOX, n = 12), DEX treatment (DOX+DEX, n = 11), transplantation of mitochondria from mice heart (DOX+MITO(Heart), n = 11), transplantation of mitochondria from human arterial blood (DOX+MITO(Blood), n = 7).

(D and E) Ejection fractions (D) and Fractional shortenings (E) were measured at 4 weeks.

(F and G) Ejection fractions (F) and Factional shortenings (G) were measured at 8 weeks.

(H) Representative left ventricular (LV) cross-sections (after 8 weeks of DOX and DEX treatment or mitochondrial transplantation) stained with hematoxylin and eosin (H&E) stain dye. Scale bars, 500 μm (n ≥ 3 per group).

(I and J) Representative images (I) and (J) quantitative analyses of Sirius red staining of heart sections in group of CON, DOX, DOX+DEX, DOX+MITO(Heart) and DOX+MITO(Blood), Scale bars, 100 μm (n ≥ 3 per group).

(K) The effects of mitochondrial transplantation on DOX-induced ROS levels (red) were evaluated by dihydroethidium (DHE) staining in cardiomyocytes. Scale bars, 50 μm (n ≥ 3 per group). All results are presented as the mean ± SEM. One-way ANOVA analysis followed by Tukey's post hoc test was applied for comparisons among multiple groups. Unpaired Student's t tests were used for comparisons between two groups. *p < 0.05, **p < 0.01, ***p < 0.001. See also Figures S11 and S12.

weekly intraperitoneally doxorubicin (5 mg/kg) doses for 4 weeks plus DEX (50 mg/kg) doses followed by 4 dose-free weeks. To observe the continuous therapy of mitochondria from different sources, the transplantation of mitochondria from the mice heart and human arterial blood was conducted at the first 2 weeks in mice with long-term doxorubicin cardiotoxicity. Echocardiographic analysis of these mice was performed to observe cardiac function. Results revealed significant decreased ventricular systolic function after doxorubicin treatment compared with control. Evidences were showed with significantly decreased overall LVEF (11.58% and 13.05%) and LVFS (8.55% and 9.29%) at 4 weeks and 8 weeks, respectively. While the cardiac function improvement was observed after DEX treatment in mice treated with doxorubicin.

Compared with doxorubicin-induced mice, the LVEF/LVFS increased by 5.78%/5.53% at 4 weeks, and increased by 5.87%/4.19% at 8 weeks. Moreover, transplantation of mitochondria isolated from mice heart tissue and human arterial blood increased LVEF/LVFS by 10.86%/6.42% and 8.95%/7.51% at 4 weeks, increased LVEF/LVFS by 9.63%/6.75% and 8.88%/6.2% at 8 weeks (Figures 11B–11G). Additionally, results from H&E staining revealed that mitochondrial transplantation reversed the significantly decreased the cardiomyocyte cross-sectional area as well as the overall cardiac volume induced by doxorubicin treatment (Figure 11H). Histological observation of Sirius red demonstrated the similar effects of transplantation of mitochondria from both mice heart tissues and human arterial blood in terms of protecting against doxorubicin-induced cardiac damage. Briefly, doxorubicin administration significantly increased the collagen areas of mice heart, which could be significantly inhibited by DEX and mitochondrial transfer (Figures 11I and 11J). In addition, we detected the ROS production by using DHE staining. Compared with mice that were treated with doxorubicin alone, mice that treated with DEX and mitochondria transfer had significantly decreased DHE fluorescence density (Figure 11K).

Finally, the effect of the glutamine supplementation was detected on the long-term effect doxorubicin-induced cardiotoxicity. Specifically, the mice received weekly intraperitoneally doxorubicin (5 mg/kg) doses for 4 weeks followed by 4 dose-free weeks. Then the doxorubicin-treated mice were treated with or without 4% glutamine in their drinking water. Next, cardiac function was assessed by echocardiography at 4 weeks and 8 weeks, respectively. Doxorubicin treatment substantially reduced the left LVEF and LVFS parameters in mice. However, the cardiac function improvement was not observed after glutamine supplementation, showing with significant decreased LVEF and LVFS in comparison with control (Figures S12A and S12B). These findings also demonstrated that mitochondrial transplantation effectively ameliorated doxorubicin-induced cardiac remodeling by glutamine metabolism activation, which could not be replaced only with glutamine supplementation.

DISCUSSION

Mitochondrial injury has been demonstrated as a critical factor in doxorubicin-induced cardiotoxicity. Our present study shows that doxorubicin-induced impairment of mitochondrial structure and function activates apoptotic signaling, increases ROS production, impairs OXPHOS, and results in cardiomyocyte death and systolic dysfunction. Whereas, transplantation of viable mitochondria inhibits these deleterious effects and preserves cardiac function in doxorubicin-treated mice. Specifically, we observed enhanced mitochondrial dynamics and respiration as well as reduced cardiomyocyte apoptosis and ROS production after mitochondrial transplantation. Mitochondria isolated from various sources, including mouse hearts, mouse and human arterial blood, and iPSC-CMs, exert similar cardioprotective effects. Mechanically, the metabolic changes induced by mitochondrial transplantation in the doxorubicin-treated heart, which include the activation of glutamine and glutamate metabolism, sere as the working mechanism of mitochondrial transplantation. Our present study firstly shows that targeting the mitochondrial damage induced by doxorubicin cardiotoxicity by mitochondrial transplantation might be a feasible strategy to prevent/treat doxorubicin-induced cardiac injury. Besides, the optimal source for mitochondria isolation was determined, which provides feasible way to obtain required mitochondria sources, especially from arterial blood.

Our study reveals mitochondrial transplantation as an innovative approach to specifically prevent doxorubicin-induced mitochondrial dysfunction. The cardioprotective effects of replacing damaged mitochondria via mitochondrial transplantation extend beyond cardiotoxicity. We have previously shown that transplantation with mitochondria modified to activate ALDH2 limits infarction size and ischemia/reperfusion injury in mice.[26] During ischemia, complex cellular responses cause extensive damage to cardiomyocytes. Because the myocardial niche regulates the retention, activity, and internalization of mitochondria after transplantation, ischemia-induced cardiomyocyte injury greatly reduces the integrity of the myocardium and therefore makes mitochondrial transplantation more challenging. Additionally, the innate immune response that occurs during ischemia/reperfusion injury is another threat to the transplanted mitochondria. Therefore, enhanced mitochondrial activity is essential to ensure the successful transplantation of viable, respiratory-competent mitochondria. However, compared with ischemia, doxorubicin treatment results in less extensive damage to the myocardium, thus providing a less hostile microenvironment for mitochondrial transplantation. Therefore, this study does not include additional mitochondrial modifications, such as ALDH2 activation, because substantial cardioprotective effects have been observed with mitochondrial transplantation alone. Nonetheless, ALDH2 activation in mitochondria may enhance the cardioprotective effects of mitochondrial transplantation in response to doxorubicin-induced cardiotoxicity. However, additional studies are warranted.

Here, we have aimed to find the optimal source of mitochondria for transplantation. Song et al.[33] have contradicted the traditional idea that mitochondria are usually located in the cytoplasm. Their results have verified the existence of circulating mitochondria in human and animal blood, which may function as novel mediators for cell-cell communication and homeostasis. In fact, platelets have been suggested as the source of these mitochondria in the blood.[16,34] These findings support our hypothesis that arterial blood may be an optimal source and delivery pathway for mitochondrial transplantation. In this study, we have developed an innovative method to isolate mitochondria from human and mouse arterial blood and have confirmed the purity of the isolated mitochondria (up to 80–90%). We have also compared the therapeutic effects between these mitochondria and others isolated from various source. Our results have demonstrated that mitochondria isolated from both human and mouse arterial blood significantly improve the overall LVEF and LVFS of doxorubicin-treated mice. These findings further indicate that blood may be a convenient source of mitochondria for transplantation. It is known that non-autologous, cell-based therapies may cause an immune response. Therefore, autologous mitochondria may be a better choice for transplantation. Nonetheless, our results have demonstrated that mitochondria isolated from both human and mouse sources exhibit great therapeutic potential for treating doxorubicin-induced cardiotoxicity, implying that mitochondrial therapy was not limited to autologous transplantation. We have further validated this using mitochondria isolated from different tissues, including mouse hearts and blood as well as human iPSC-CMs and blood. All of these

mitochondria ameliorate doxorubicin-induced cardiac injury and do not exhibit tissue specificity, demonstrating successful circumvention of the immune and inflammatory responses.

There are few reports on how mitochondrial transplantation plays a role in cardiac protection, but the underlying mechanism remains unclear. Our findings have demonstrated that glutamine metabolism is significantly activated after mitochondrial transplantation in the doxorubicin-treated mouse heart. Figure 7 showed that mitochondrial respiration was activated while glycolysis was decreased by mitochondrial transplantation. These data indicated that the limited pyruvate production from glycolysis was inefficient in sustaining the TCA cycle and subsequently OXPHOS in mitochondria. Then we asked what might be the major factor responsible for sustaining TCA cycle? As the most abundant circulating amino acid, increased levels of glutamine were observed in doxorubicin-treated heart with mitochondrial transplantation. Upon entry into the cell via transporters, glutamine is converted by mitochondrial glutaminases to an ammonium ion and glutamate, which is further catabolized through the α-ketoglutarate and glutathione (GSH) metabolic pathways.[35] Glutamine carbons predominantly go through the α-ketoglutarate pathway to enter the TCA cycle, where ATP is generated through the production of nicotinamide adenine dinucleotide (NADH) and flavin adenine dinucleotide (FADH2). The increased glutamine might result in metabolic rewriting, which is responsible for the activation of mitochondrial respiratory in doxorubicin-treated heart after mitochondrial transfer. This metabolic rewriting might result in the increased expression of IDH2 CS, which is responsible for TCA cycle. Consistently, the protein expression of GLS, which facilitates the conversion of glutamine to glutamate, is significantly upregulated after mitochondrial transplantation in the doxorubicin-treated heart. Furthermore, GSH metabolism controls the levels of mitochondrial ROS.[36] In this study, our findings have revealed that mitochondrial transplantation improves respiratory capacity and inhibits total ROS formation in doxorubicin-treated cardiomyocytes. Therefore, we conclude that glutamine metabolism could help scavenge cellular ROS and induce the changes of pATM, MnSOD, and OGG1. Consequently, the gene responsible for mitogenesis and mitochondrial dynamics was upregulated, including Tfam, Ppargc1b, and Opa1. Additional *in vitro* and *in vivo* experiments using glutamine antagonists, DON and JHU083, have demonstrated that inhibition of glutamine metabolism diminishes the cardioprotective effects of mitochondrial transplantation in cardiomyocytes after doxorubicin treatment. These results provide a theoretical basis and demonstrate the role of metabolic regulation following mitochondrial transplantation for the successful treatment of doxorubicin-induced cardiotoxicity. The aforementioned results collectively hint an important role of glutamine metabolism activation on the observed beneficial effects of mitochondria transfer in our model.

Current interventions (e.g., Mito-Q, carvedilol, berberine, and dexrazoxane) to reduce doxorubicin-induced cardiotoxicity predominantly involve the use of antioxidants to eliminate ROS and preserve mitochondrial function.[37–43] For example, carvedilol, a nonselective β-adrenergic receptor antagonist, displayed potent antioxidant protection of cardiac mitochondria. Carvedilol and its metabolites improved cardiac mitochondrial function, including augmenting calcium loading capacity, during sub-chronic doxorubicin treatment.[44] CoQ10 is one of the most important antioxidants in cardiac cells, providing effective protection against anthracycline induced oxidative damage and the development of cardiomyopathy.[45] In addition, the dexrazoxane is the only FDA-approved protective therapy against doxorubicin toxicity. The mechanism of cardio-protection by dexrazoxane was thought to be mediated by iron chelation, inhibition of topoisomerase 2-β, thus indirectly through an antioxidant effect.[7] Whereas, our present study proposed the mitochondria transplantation as the potential therapeutic strategy in doxorubicin-treated heart by activating the metabolic remodeling. Except for the antioxidative role, mitochondrial transplantation induced the metabolic rewriting of doxorubicin-treated heart by glutamine metabolic activation, which significantly enhanced respiratory capacity of cardiomyocytes. Specifically, our study demonstrated the significant increased levels of glutamine and GLS. Glutamine is the most abundant circulating amino acid, which plays an anaplerotic role by replenishing TCA cycle intermediates for the production of reducing equivalents that drive the mitochondrial respiratory chain. Furthermore, the expression of genes responsible for mitochondrial biogenesis and dynamics was activated by mitochondrial transplantation. Our Figure S5 demonstrated the activated mitophagy induced by mitochondrial transplantation. These findings indicated the increased elimination of damaged mitochondrial proteins or parts of the mitochondrial network by mitophagy and replenish components by adding protein and lipids through biogenesis, collectively resulting in mitochondrial turnover. Future studies are needed to compare the therapeutic efficacy of mitochondria transplantation versus currently used anti-oxidant therapies as well as dexrazoxane medication, and to explore if mitochondria transplantation on top of currently used anti-oxidant therapies as well as dexrazoxane medication could have significant synergic effects or not.

The dynamic properties of mitochondria—including their fusion, fission, and degradation—are critical for their optimal function in maintenance of a healthy and functional mitochondrial network. The interplay of fusion and fission confers widespread benefits on mitochondria, including efficient transport, increased homogenization of the mitochondrial population, and efficient OXPHOS.[46] The mRNA expression of genes responsible for mitochondrial biogenesis (*Tfam*, *Ppargc1a*, *Ppargc1b*, and *Nrf1*) and dynamics (*Mfn1*, *Mfn2*, *Opa1*, *Fis1*, *Mff*, *Mief1*, and *Mief2*) assessed in our study therefore reflected the mitochondrial dynamic function. Doxorubicin treatment significantly inhibited the mRNA expression of *Tfam*, *Ppargc1b*, *Opa1*, and *Mief2*, which indicated the mitochondrial injury induced by doxorubicin treatment partly resulted from mitochondrial biogenesis and dynamics. However, mitochondrial biogenesis and dynamics were reactivated after doxorubicin treatment and mitochondrial transplantation, evidenced with significantly increased mRNA expression of *Ppargc1b* and *Opa1*. These pathways reactivated by mitochondrial transplantation work to eliminate damaged mitochondrial proteins or parts of the mitochondrial network by mitophagy and renew components by adding protein and lipids through biogenesis, collectively resulting in mitochondrial turnover. Altogether, mitochondrial transplantation significantly improved mitochondrial dysfunction induced by doxorubicin treatment.

Though the clearance and self-repair mechanisms of injured mitochondria exist, we suggested that the mitochondrial self-repair and proliferation was inefficient to inhibit the development and accumulation of doxorubicin-induced cardiotoxicity. As shown in Figures S5A–S5C,

mitophagy was activated in mice heart post mitochondrial transplantation, indicating that the elimination of damaged mitochondria was accelerated by mitophagy-like machinery. More importantly, the present study demonstrated that mitochondrial transplantation significantly enhanced mitochondrial self-repair and proliferation in comparison with that of doxorubicin-treated heart without mitochondrial transfer, evidenced by restored mitochondrial biogenesis and dynamics. In addition, recovery of mitochondrial respiratory induced by mitochondrial transplantation in doxorubicin-treated heart was dependent on the activation of glutamine metabolism. These results suggested that increased glutamine resulted in metabolic rewriting of doxorubicin-treated cardiomyocytes. The generation of the antioxidant GSH could also be activated by glutamine metabolism. GSH regulated of the intracellular redox potential and exhibited protective effect against oxidative injury. Our study thus suggested that besides promoting mitochondrial self-repair, mitochondrial transplantation in doxorubicin-treated heart also stimulated additional rescue factors, including mitochondrial biogenesis, dynamics, and metabolic rewriting. It is necessary to restore doxorubicin-induced cardiac injury by mitochondrial transplantation.

Cardiac muscle contraction is generated at the molecular level by cyclical, adenosine 5′-triphosphate (ATP)-driven actin-myosin interactions. Chemical energy, supplied by hydrolysis of MgATP, is converted into mechanical work, force, and shortening.[47,48] As the important driver of cardiac contraction, ATP was regulated by mitochondrial oxidative function. Our present study demonstrated that mitochondrial OXPHOS of doxorubicin-treated cardiomyocytes was activated by mitochondrial transplantation (Figure 7). Then the changes of OXPHOS directly regulated cardiac function and contractility. The cardiac contractility was shown in Figures 3E–3J. This contractile response was evaluated in cardiomyocytes isolated from doxorubicin-treated mice with or without mitochondrial transplantation. Results showed that doxorubicin treatment caused contractile dysfunction in the cardiomyocytes, which was reversed by mitochondrial transplantation. Specifically, doxorubicin treatment induced an overall decrease in the maximal velocity of shortening/relengthening ($\pm$dl/dt) and peak shortening (% cell lengthening) in the cardiomyocytes; however, these were increased after mitochondrial transplantation (Figures 3F–3H). Likewise, doxorubicin treatment caused an elevated TPS-s in the cardiomyocytes, which was decreased after mitochondrial transplantation (Figures 3I and 3J). We concluded that the changes of OXPHOS directly regulated cardiac function and contractility and can be regulated by the mitochondrial transplantation.

Limitations of the study

Mitochondrial transplantation ameliorates doxorubicin-induced myocardial injury by improving cardiomyocyte contractility and mitochondrial OXPHOS as well as by inhibiting cardiomyocyte apoptosis and ROS production. These findings demonstrate the therapeutic potential of mitochondrial transplantation. A limitation of this study is that we have failed to observe any dynamic changes after mitochondrial transplantation *in vivo*. However, our previous study has shown that the dynamic internalization of exogenous mitochondria by cardiomyocytes has cardioprotective effects that are mediated by mitochondrial membrane potential-induced fusion.[26] In this study, the internalization of exogenous mitochondria may have protected cardiomyocytes from stress in response to doxorubicin treatment. The activation of glutamine metabolism following mitochondrial transplantation may then promote this mitochondrial internalization, possibly explaining the observed resistance in cellular stress, including reduced apoptotic and ROS signaling, after mitochondrial transplantation. The present study has mainly focused on demonstrating the translational application of mitochondrial transplantation as well as finding the most effective method for mitochondrial isolation. Therefore, our future studies will include intracellular mitochondrial dynamics. Furthermore, it is to note that limited number of models was used in the current study (*in vitro*: 1 cell line, *in vivo*: 1 mouse model). Future studies are needed to validate whether it is possible to extend present study results with additional models. In addition, the present strategy of mitochondrial transplantation in mice showed weak feasibility in humans. To promote the clinical application of mitochondrial transplantation, we will explore non-invasive transplantation of mitochondria in our model as soon as possible. It is to note that the current data could not explain whether mitochondria directly rescue cardiomyocytes or indirectly activate other cells for beneficial protection. Future studies are needed to address this issue.

STAR★METHODS

Detailed methods are provided in the online version of this paper and include the following:

- KEY RESOURCES TABLE
- RESOURCE AVAILABILITY
  - Lead contact
  - Materials availability
  - Data and code availability
- EXPERIMENTAL MODEL AND STUDY PARTICIPANT DETAILS
  - Cell lines
  - Animal model
  - Human subject
- METHOD DETAILS
  - Cardiomyocyte isolation
  - Doxorubicin treatment and mitochondrial transplantation of cultured cells
  - TEM staining assay

- Mechanical function assay
- Plasmid and siRNA transfection
- Bioenergetics assay
- Living cell imaging
- Reactive oxygen species analysis
- Mitochondria isolation from arterial blood
- Mitochondria isolation from mouse heart and cells
- Echocardiography analysis
- Mitotracker Green/deep red staining
- TUNEL assay
- Tumor inhibition
- Total RNA extraction
- mRNA library construction
- Western blot analysis
- Flow cytometric analysis
- Application of glutamine blockade
- Histology
- Metabolites extraction
- LC-MS/MS analysis
- Data preprocessing and annotation of LC-MS/MS analysis

- QUANTIFICATION AND STATISTICAL ANALYSIS
  - Statistical analysis

SUPPLEMENTAL INFORMATION

Supplemental information can be found online at https://doi.org/10.1016/j.isci.2023.107790.

ACKNOWLEDGMENTS

X. S., H. C., R. G., and Y.H. contributed equally to this work. This work was supported by grants from the National Natural Science Foundation of China (81900353, 82270264, T2288101, and 82130010) and the National Science Fund for Distinguished Young Scholars (817200010). Our data analysis of LC-MS/MS was assisted by Biotree Biotech Co., Ltd. (Shanghai, China). The graphic abstract was designed by Dipl.-Ing. Yang Yang.

AUTHOR CONTRIBUTIONS

X.S. and H.C. designed the research. R.G., Y.H., Y.Q., and H.Y. developed the experimental methods, performed most experiments, and analyzed the data. X.W., S.H., J.Z., and P.W. provided technical support. Y.Z. and J.G. supervised this work. X.S. wrote the manuscript. K.H. and A.S. edited the manuscript.

DECLARATION OF INTERESTS

The authors declare no conflict of interests.

Received: November 27, 2022
Revised: August 14, 2023
Accepted: August 28, 2023
Published: September 1, 2023

REFERENCES

1. Bonadonna, G., Monfardini, S., De Lena, M., Fossati-Bellani, F., and Beretta, G. (1970). Phase I and preliminary phase II evaluation of adriamycin (NSC 123127). Cancer Res. *30*, 2572–2582.
2. Hortobágyi, G.N. (1997). Anthracyclines in the treatment of cancer. An overview. Drugs *54*, 1–7. https://doi.org/10.2165/00003495-199700544-00003.
3. Swain, S.M., Whaley, F.S., and Ewer, M.S. (2003). Congestive heart failure in patients treated with doxorubicin: a retrospective analysis of three trials. Cancer *97*, 2869–2879. https://doi.org/10.1002/cncr.11407.
4. Kilickap, S., Barista, I., Akgul, E., Aytemir, K., Aksoy, S., and Tekuzman, G. (2007). Early and late arrhythmogenic effects of doxorubicin. South. Med. J. *100*, 262–265. https://doi.org/10.1097/01.smj.0000257382.89910.fe.
5. Fitter, W., deSa, D.J., and Pai, K.R. (1981). Adriamycin cardiotoxicity: report of an unusual case with features resembling endomyocardial fibrosis. J. Clin. Pathol. *34*, 602–605. https://doi.org/10.1136/jcp.34.6.602.
6. Jordan, J.H., Castellino, S.M., Meléndez, G.C., Klepin, H.D., Ellis, L.R., Lamar, Z., Vasu, S., Kitzman, D.W., Ntim, W.O., Brubaker, P.H., et al. (2018). Left Ventricular Mass Change After Anthracycline Chemotherapy. Circ. Heart Fail. *11*, e004560. https://doi.org/10.1161/CIRCHEARTFAILURE.117.004560.
7. Wallace, K.B., Sardão, V.A., and Oliveira, P.J. (2020). Mitochondrial Determinants of Doxorubicin-Induced Cardiomyopathy. Circ.

Res. *126*, 926–941. https://doi.org/10.1161/CIRCRESAHA.119.314681.

8. Davies, K.J., and Doroshow, J.H. (1986). Redox cycling of anthracyclines by cardiac mitochondria. I. Anthracycline radical formation by NADH dehydrogenase. J. Biol. Chem. *261*, 3060–3067.
9. Solem, L.E., Henry, T.R., and Wallace, K.B. (1994). Disruption of mitochondrial calcium homeostasis following chronic doxorubicin administration. Toxicol. Appl. Pharmacol. *129*, 214–222. https://doi.org/10.1006/taap.1994.1246.
10. Ichikawa, Y., Ghanefar, M., Bayeva, M., Wu, R., Khechaduri, A., Naga Prasad, S.V., Mutharasan, R.K., Naik, T.J., and Ardehali, H. (2014). Cardiotoxicity of doxorubicin is mediated through mitochondrial iron accumulation. J. Clin. Invest. *124*, 617–630. https://doi.org/10.1172/JCI72931.
11. Marechal, X., Montaigne, D., Marciniak, C., Marchetti, P., Hassoun, S.M., Beauvillain, J.C., Lancel, S., and Neviere, R. (2011). Doxorubicin-induced cardiac dysfunction is attenuated by ciclosporin treatment in mice through improvements in mitochondrial bioenergetics. Clin. Sci. *121*, 405–413. https://doi.org/10.1042/CS20110069.
12. Zhang, S., Liu, X., Bawa-Khalfe, T., Lu, L.S., Lyu, Y.L., Liu, L.F., and Yeh, E.T.H. (2012). Identification of the molecular basis of doxorubicin-induced cardiotoxicity. Nat. Med. *18*, 1639–1642. https://doi.org/10.1038/nm.2919.
13. Hoshino, A., Mita, Y., Okawa, Y., Ariyoshi, M., Iwai-Kanai, E., Ueyama, T., Ikeda, K., Ogata, T., and Matoba, S. (2013). Cytosolic p53 inhibits Parkin-mediated mitophagy and promotes mitochondrial dysfunction in the mouse heart. Nat. Commun. *4*, 2308. https://doi.org/10.1038/ncomms3308.
14. Jing, X., Yang, J., Jiang, L., Chen, J., and Wang, H. (2018). MicroRNA-29b Regulates the Mitochondria-Dependent Apoptotic Pathway by Targeting Bax in Doxorubicin Cardiotoxicity. Cell. Physiol. Biochem. *48*, 692–704. https://doi.org/10.1159/000491896.
15. Kumar, D., Kirshenbaum, L., Li, T., Danelisen, I., and Singal, P. (1999). Apoptosis in isolated adult cardiomyocytes exposed to adriamycin. Ann. N. Y. Acad. Sci. *874*, 156–168. https://doi.org/10.1111/j.1749-6632.1999.tb09233.x.
16. Ma, H., Jiang, T., Tang, W., Ma, Z., Pu, K., Xu, F., Chang, H., Zhao, G., Gao, W., Li, Y., and Wang, Q. (2020). Transplantation of platelet-derived mitochondria alleviates cognitive impairment and mitochondrial dysfunction in db/db mice. Clin. Sci. *134*, 2161–2175. https://doi.org/10.1042/CS20200530.
17. Lin, H.C., and Lai, I.R. (2013). Isolated mitochondria infusion mitigates ischemia-reperfusion injury of the liver in rats: reply. Shock *39*, 543. https://doi.org/10.1097/01.shk.0000430660.63077.7f.
18. Orfany, A., Arriola, C.G., Doulamis, I.P., Guariento, A., Ramirez-Barbieri, G., Moskowitzova, K., Shin, B., Blitzer, D., Rogers, C., Del Nido, P.J., and McCully, J.D. (2020). Mitochondrial transplantation ameliorates acute limb ischemia. J. Vasc. Surg. *71*, 1014–1026. https://doi.org/10.1016/j.jvs.2019.03.079.
19. Moskowitzova, K., Orfany, A., Liu, K., Ramirez-Barbieri, G., Thedsanamoorthy, J.K., Yao, R., Guariento, A., Doulamis, I.P., Blitzer, D., Shin, B., et al. (2020). Mitochondrial transplantation enhances murine lung viability and recovery after ischemia-reperfusion injury. Am. J. Physiol. Lung Cell Mol. Physiol. *318*, L78–L88. https://doi.org/10.1152/ajplung.00221.2019.
20. Kunecki, M., Płazak, W., Podolec, P., and Gołba, K.S. (2017). Effects of endogenous cardioprotective mechanisms on ischemia-reperfusion injury. Postepy Hig. Med. Dosw. *71*, 20–31. https://doi.org/10.5604/17322693.1228267.
21. McCully, J.D., Cowan, D.B., Pacak, C.A., Toumpoulis, I.K., Dayalan, H., and Levitsky, S. (2009). Injection of isolated mitochondria during early reperfusion for cardioprotection. Am. J. Physiol. Heart Circ. Physiol. *296*, H94–H105. https://doi.org/10.1152/ajpheart.00567.
22. McCully, J.D., Cowan, D.B., Emani, S.M., and Del Nido, P.J. (2017). Mitochondrial transplantation: From animal models to clinical use in humans. Mitochondrion *34*, 127–134. https://doi.org/10.1016/j.mito.2017.03.004.
23. Shin, B., Saeed, M.Y., Esch, J.J., Guariento, A., Blitzer, D., Moskowitzova, K., Ramirez-Barbieri, G., Orfany, A., Thedsanamoorthy, J.K., Cowan, D.B., et al. (2019). A Novel Biological Strategy for Myocardial Protection by Intracoronary Delivery of Mitochondria: Safety and Efficacy. JACC. Basic Transl. Sci. *4*, 871–888. https://doi.org/10.1016/j.jacbts.2019.08.007.
24. Kaza, A.K., Wamala, I., Friehs, I., Kuebler, J.D., Rathod, R.H., Berra, I., Ericsson, M., Yao, R., Thedsanamoorthy, J.K., Zurakowski, D., et al. (2017). Myocardial rescue with autologous mitochondrial transplantation in a porcine model of ischemia/reperfusion. J. Thorac. Cardiovasc. Surg. *153*, 934–943. https://doi.org/10.1016/j.jtcvs.2016.10.077.
25. Emani, S.M., Piekarski, B.L., Harrild, D., Del Nido, P.J., and McCully, J.D. (2017). Autologous mitochondrial transplantation for dysfunction after ischemia-reperfusion injury. J. Thorac. Cardiovasc. Surg. *154*, 286–289. https://doi.org/10.1016/j.jtcvs.2017.02.018.
26. Sun, X., Gao, R., Li, W., Zhao, Y., Yang, H., Chen, H., Jiang, H., Dong, Z., Hu, J., Liu, J., et al. (2021). Alda-1 treatment promotes the therapeutic effect of mitochondrial transplantation for myocardial ischemia-reperfusion injury. Bioact. Mater. *6*, 2058–2069. https://doi.org/10.1016/j.bioactmat.2020.12.024.
27. Doroshow, J.H., and Davies, K.J. (1986). Redox cycling of anthracyclines by cardiac mitochondria. II. Formation of superoxide anion, hydrogen peroxide, and hydroxyl radical. J. Biol. Chem. *261*, 3068–3074.
28. Cooper, M.L., Adami, H.O., Grönberg, H., Wiklund, F., Green, F.R., and Rayman, M.P. (2008). Interaction between single nucleotide polymorphisms in selenoprotein P and mitochondrial superoxide dismutase determines prostate cancer risk. Cancer Res. *68*, 10171–10177. https://doi.org/10.1158/0008-5472.CAN-08-1827.
29. Minig, V., Kattan, Z., van Beeumen, J., Brunner, E., and Becuwe, P. (2009). Identification of DDB2 protein as a transcriptional regulator of constitutive SOD2 gene expression in human breast cancer cells. J. Biol. Chem. *284*, 14165–14176. https://doi.org/10.1074/jbc.M808208200.
30. Sun, A., Zou, Y., Wang, P., Xu, D., Gong, H., Wang, S., Qin, Y., Zhang, P., Chen, Y., Harada, M., et al. (2014). Mitochondrial aldehyde dehydrogenase 2 plays protective roles in heart failure after myocardial infarction via suppression of the cytosolic JNK/p53 pathway in mice. J. Am. Heart Assoc. *3*, e000779. https://doi.org/10.1161/JAHA.113.000779.
31. Sampath, H., and Lloyd, R.S. (2019). Roles of OGG1 in transcriptional regulation and maintenance of metabolic homeostasis. DNA Repair *81*, 102667. https://doi.org/10.1016/j.dnarep.2019.102667.
32. Forman, H.J., Zhang, H., and Rinna, A. (2009). Glutathione: overview of its protective roles, measurement, and biosynthesis. Mol. Aspect. Med. *30*, 1–12. https://doi.org/10.1016/j.mam.2008.08.006.
33. Song, X., Hu, W., Yu, H., Wang, H., Zhao, Y., Korngold, R., and Zhao, Y. (2020). Existence of Circulating Mitochondria in Human and Animal Peripheral Blood. Int. J. Mol. Sci. *21*, 2122. https://doi.org/10.3390/ijms21062122.
34. Boudreau, L.H., Duchez, A.C., Cloutier, N., Soulet, D., Martin, N., Bollinger, J., Paré, A., Rousseau, M., Naika, G.S., Lévesque, T., et al. (2014). Platelets release mitochondria serving as substrate for bactericidal group IIA-secreted phospholipase A2 to promote inflammation. Blood *124*, 2173–2183. https://doi.org/10.1182/blood-2014-05-573543.
35. Altman, B.J., Stine, Z.E., and Dang, C.V. (2016). From Krebs to clinic: glutamine metabolism to cancer therapy. Nat. Rev. Cancer *16*, 749. https://doi.org/10.1038/nrc.2016.114.
36. Krebs, H.A. (1935). Metabolism of amino-acids: The synthesis of glutamine from glutamic acid and ammonia, and the enzymic hydrolysis of glutamine in animal tissues. Biochem. J. *29*, 1951–1969. https://doi.org/10.1042/bj0291951.
37. Hasinoff, B.B., Patel, D., and Wu, X. (2003). The oral iron chelator ICL670A (deferasirox) does not protect myocytes against doxorubicin. Free Radic. Biol. Med. *35*, 1469–1479. https://doi.org/10.1016/j.freeradbiomed.2003.08.005.
38. Deng, S., Yan, T., Jendrny, C., Nemecek, A., Vincetic, M., Gödtel-Armbrust, U., and Wojnowski, L. (2014). Dexrazoxane may prevent doxorubicin-induced DNA damage via depleting both topoisomerase II isoforms. BMC Cancer *14*, 842. https://doi.org/10.1186/1471-2407-14-842.
39. Kametani, R., Miura, T., Harada, N., Shibuya, M., Wang, R., Tan, H., Fukagawa, Y., Kawamura, S., and Matsuzaki, M. (2006). Carvedilol inhibits mitochondrial oxygen consumption and superoxide production during calcium overload in isolated heart mitochondria. Circ. J. *70*, 321–326. https://doi.org/10.1253/circj.70.321.
40. Oliveira, P.J., Esteves, T., Rolo, A.P., Palmeira, C.M., and Moreno, A.J.M. (2004). Carvedilol inhibits the mitochondrial permeability transition by an antioxidant mechanism. Cardiovasc. Toxicol. *4*, 11–20. https://doi.org/10.1385/ct:4:1:11.
41. Xiong, C., Wu, Y.Z., Zhang, Y., Wu, Z.X., Chen, X.Y., Jiang, P., Guo, H.C., Xie, K.R., Wang, K.X., and Su, S.W. (2018). Protective effect of berberine on acute cardiomyopathy associated with doxorubicin treatment. Oncol. Lett. *15*, 5721–5729. https://doi.org/10.3892/ol.2018.8020.
42. Zhao, Y., Tian, X., Liu, G., Wang, K., Xie, Y., and Qiu, Y. (2019). Berberine protects myocardial cells against anoxia-reoxygenation injury via p38 MAPK-mediated NF-kappaB signaling pathways. Exp. Ther. Med. *17*, 230–236. https://doi.org/10.3892/etm.2018.6949.
43. Lue, Y., Gao, C., Swerdloff, R., Hoang, J., Avetisyan, R., Jia, Y., Rao, M., Ren, S., Atienza,

V., Yu, J., et al. (2018). Humanin analog enhances the protective effect of dexrazoxane against doxorubicin-induced cardiotoxicity. Am. J. Physiol. Heart Circ. Physiol. *315*, H634–H643. https://doi.org/10.1152/ajpheart.00155.2018.

44. Santos, D.L., Moreno, A.J.M., Leino, R.L., Froberg, M.K., and Wallace, K.B. (2002). Carvedilol protects against doxorubicin-induced mitochondrial cardiomyopathy. Toxicol. Appl. Pharmacol. *185*, 218–227. https://doi.org/10.1006/taap.2002.9532.
45. Conklin, K.A. (2005). Coenzyme q10 for prevention of anthracycline-induced cardiotoxicity. Integr. Cancer Ther. *4*, 110–130. https://doi.org/10.1177/1534735405276191.
46. Chan, D.C. (2020). Mitochondrial Dynamics and Its Involvement in Disease. Annu. Rev. Pathol. *15*, 235–259. https://doi.org/10.1146/annurev-pathmechdis-012419-032711.
47. Regnier, M., Rivera, A.J., Chen, Y., and Chase, P.B. (2000). 2-deoxy-ATP enhances contractility of rat cardiac muscle. Circ. Res. *86*, 1211–1217. https://doi.org/10.1161/01.res.86.12.1211.
48. Powers, J.D., Yuan, C.C., McCabe, K.J., Murray, J.D., Childers, M.C., Flint, G.V., Moussavi-Harami, F., Mohran, S., Castillo, R., Zuzek, C., et al. (2019). Cardiac myosin activation with 2-deoxy-ATP via increased electrostatic interactions with actin. Proc. Natl. Acad. Sci. USA *116*, 11502–11507. https://doi.org/10.1073/pnas.1905028116.
49. Ackers-Johnson, M., Li, P.Y., Holmes, A.P., O'Brien, S.M., Pavlovic, D., and Foo, R.S. (2016). A Simplified, Langendorff-Free Method for Concomitant Isolation of Viable Cardiac Myocytes and Nonmyocytes From the Adult Mouse Heart. Circ. Res. *119*, 909–920. https://doi.org/10.1161/CIRCRESAHA.116.309202.
50. Sun, X., Zhu, H., Dong, Z., Liu, X., Ma, X., Han, S., Lu, F., Wang, P., Qian, S., Wang, C., et al. (2017). Mitochondrial aldehyde dehydrogenase-2 deficiency compromises therapeutic effect of ALDH bright cell on peripheral ischemia. Redox Biol. *13*, 196–206. https://doi.org/10.1016/j.redox.2017.05.018.
51. Leone, R.D., Zhao, L., Englert, J.M., Sun, I.M., Oh, M.H., Sun, I.H., Arwood, M.L., Bettencourt, I.A., Patel, C.H., Wen, J., et al. (2019). Glutamine blockade induces divergent metabolic programs to overcome tumor immune evasion. Science *366*, 1013–1021. https://doi.org/10.1126/science.aav2588.

STAR★METHODS

KEY RESOURCES TABLE

REAGENT or RESOURCE	SOURCE	IDENTIFIER
Antibodies		
Rabbit monoclonal anti-CS	Cell Signaling Technology	Cat#14309S
Rabbit monoclonal anti-VDAC	Cell Signaling Technology	Cat#4661S
Rabbit polyclonal anti-Bax	Cell Signaling Technology	Cat#2772S
Rabbit monoclonal anti-Bcl2	Cell Signaling Technology	Cat#3498S
Rabbit polyclonal anti-Caspase-3	Cell Signaling Technology	Cat#9662S
Rabbit polyclonal anti-NDUFAB1	Abcam	Cat#ab181021
Rabbit polyclonal anti-SDHD	Abcam	Cat#ab189945
Rabbit polyclonal anti-SDHA	Abcam	Cat#ab137756
Goat polyclonal anti-OGG1	Abcam	Cat#ab62826
Rabbit monoclonal anti-SOD2/MnSOD	Abcam	Cat#ab68155
Rabbit KGA/GAC (GLS) Polyclonal antibody	Proteintech	Cat #12855-1-AP
FITC anti-mouse/human CD11b	BioLegend	Cat#101206
PerCP/Cyanine5.5 anti-mouse CD45	BioLegend	Cat#103132
APC anti-mouse Ly-6G	BioLegend	Cat#127614
Zombie Aqua™ Fixable Viability Kit	BioLegend	Cat# 423102
Mouse monoclonal anti-*p*-ATM	Sigma-Aldrich	Cat#05-740
Rabbit monoclonal anti-TOM20	Cell Signaling Technology	Cat# 42406S
Monoclonal Mouse Anti-glyceraldehyde-3-phosphate Dehydrogenase (GAPDH)	Aksomics	KC-5G4
HRP-conjugated Monoclonal Mouse Anti-beta Actin	Aksomics	KC-5A08
Mouse monoclonal ant-Cardiac Troponin T (cTnT)	Abcam	Cat#ab8295
PINK1 Rabbit pAb	ABclonal	Cat#A7131
Parkin Antibody	Affinity	Cat#AF0235
Biological samples		
Male C57BL/6 mice	Cavens Biogle Model Animal Research Co., Ltd.	N/A
Cox4i1-GFP mice	Shanghai Model Organisms Center, Inc.	N/A
Chemicals, peptides, and recombinant proteins		
Laminin (murine)	Thermo Scientific	Cat#23017-15
M199 Medium	Sigma-Aldrich	Cat#M4530
ITS supplement	Sigma-Aldrich	Cat#I3146
Chemically defined lipid concentrate	Thermo Scientific	Cat#11905-031
Penicillin-Streptomycin	Thermo Scientific	Cat#15070-063
Collagenase 2	Worthington	Cat#LS004176
Collagenase 4	Worthington	Cat#LS004188
Protease XIV	Sigma-Aldrich	Cat#P5147
DMEM (1X)	Gibco	Cat#11965092
Fetal bovine serum (FBS)	Bioind	Cat#04-001-1A
MitoTracker Green	Cell Signaling Technology	Cat#9074S

(*Continued on next page*)

Continued

REAGENT or RESOURCE	SOURCE	IDENTIFIER
MitoTracker Deep Red	Cell Signaling Technology	Cat#8778S
RIPA lysis buffer	Beyotime Biotechnology	Cat#P0013B
Dihydroethidium	Beyotime Biotechnology	Cat#S0063
Reactive Oxygen Species Assay Kit (DCFH-DA)	Beyotime Biotechnology	Cat#S0033S
Mitochondrial Membrane Potential Assay Kit with TMRE	Beyotime Biotechnology	Cat#C2001S
Methanol (HPLC, ≥99.9%)	Sigma-Aldrich	Cat#34860
L-Glutamine	Sigma-Aldrich	Cat#G8540-100G
6-Diazo-5-oxo-L-norleucine (DON)	Selleck	Cat#S8620
JHU-083	Selleck	Cat#S8891
MitoSOX	Thermo Scientific	Cat#M36008
One Step TUNEL Apoptosis Assay Kit	Beyotime Biotechnology	Cat#C1090/Cat#C1088
Tissue Mitochondria Isolation Kit	Beyotime Biotechnology	Cat#C3606
Cell Mitochondria Isolation Kit	Beyotime Biotechnology	Cat#C3601
Seahorse XF Cell Mito Stress Test Kit	Agilent	Cat#103010-100
mTeSR1 basal medium	STEMCELLTECHNOLOGY	Cat#85850
mTeSR1 5xsupplement	STEMCELLTECHNOLOGY	Cat#85852
RPMI 1640	Thermo Scientific	Cat#11875093
B27 supplement with insulin	Thermo Scientific	Cat#17504044
CHIR-99021 (CT99021)	Selleckchem	Cat#S1263
IWR-1	MilliporeSigma	Cat#I0161
Critical commercial assays		
Liquid chromatography-tandem mass spectrometry (LC-MS/MS)	Shanghai Biotree biotech CO., Ltd.	N/A
Deposited data		
Metabolomics data	This paper	MTBLS7989
Experimental models: Cell lines		
H9C2	Shanghai Zhong Qiao Xin Zhou Biotechnology Co., Ltd.	Cat#ZQ0102
EMT6	Shanghai Zhong Qiao Xin Zhou Biotechnology Co., Ltd.	Cat#ZQ0737
Human Induced Pluripotent Stem Cells	Shanghai Zhong Qiao Xin Zhou Biotechnology Co., Ltd.	Cat#DF-GMP-ZB11ALD-G-QX-22
Oligonucleotides		
si-*r*-Ogg1_001 (CTAAGACATCGCAGACTAA)	GUANGZHOU RIBOBIO CO., LTD.	Cat# siG2302270415139834
si-*r*-Ogg1_002(GTGCTAAAGCCATCCTAGA)	GUANGZHOU RIBOBIO CO., LTD.	Cat# siG2302270415140926
si-*r*-Ogg1_003(GCTGACTGCATCTGCTTAA)	GUANGZHOU RIBOBIO CO., LTD.	Cat# siG2302270415142018
si-*r*-Gls_001(CCACATAATCCGATGGTAA)	GUANGZHOU RIBOBIO CO., LTD.	Cat# siG170301034449
si-*r*-Gls_002(GCAACAGTGTTAAAGGAAT)	GUANGZHOU RIBOBIO CO., LTD.	Cat# siG170301034644
si-*r*-Gls_003 (GGGAACTGAGTATGTGCAT)	GUANGZHOU RIBOBIO CO., LTD.	Cat# siG170301034757
Software and algorithms		
ImageJ software (version 4.0)	NIH	https://imagej.nih.gov/ij/
FlowJo (v10)	BD Biosciences	https://www.flowjo.com/
Seahorse wave software	Seahorse bioscience	https://www.agilent.com.cn/
GraphPad Prism version 8	Graphpad Software Inc.	https://www.graphpad.com/scientific-software/prism/

RESOURCE AVAILABILITY

Lead contact

Further information and requests for resources and reagents should be directed to and will be fulfilled by the lead contact, Aijun Sun (sun.aijun@zs-hospital.sh.cn).

Materials availability

This study did not generate new unique reagents.

Data and code availability

- The LC-MS/MS data were deposited in the MetaboLights repository (www.ebi.ac.uk/metabolights/) under the accession number MTBLS7989. Data generated and/or analyzed in this study, excluding identifying personal information, are available from the lead author Aijun Sun (sun.aijun@zs-hospital.sh.cn) with reasonable request to protect research participant privacy.
- This study did not generate new original code.
- Any additional information required to reanalyze the data reported in this work paper is available from the lead contact upon request.

EXPERIMENTAL MODEL AND STUDY PARTICIPANT DETAILS

Cell lines

H9C2 rat cardiomyoblast cells (Cat#ZQ0102), EMT6 (Cat#ZQ0737) cells and iPSCs (Cat#DF-GMP-ZB11ALD-G-QX-22) were obtained from Shanghai Zhong Qiao Xin Zhou Biotechnology Co., Ltd. H9C2 and EMT6 cells were cultured in Dulbecco's Modified Eagle's Medium (DMEM) (Gibco) contained 10% Fetal bovine serum and penicillin (100 units/mL). iPSCs was maintained in mTeSR1 basal medium and deafferented in RPMI1640 [supplemented with B27 minus insulin (Invitrogen)]. 6 mM CHIR99021 and 5 mM IWR1 (Sigma-Aldrich) was added to the differentiation medium at 0-1day and 3–5 days respectively to induce iPSCs-CM. The Langendorff-free method was used for the isolation of adult primary cardiomyocytes. The isolated cardiomyocytes were plated onto a laminin-precoated culture dish (5 μg/mL). All above cells were maintained in a humidified culture incubator (Thermo Fisher Scientific, Waltham, MA, USA) under 5% CO2 at 37°C.

Animal model

6–8 weeks old male and female C57BL/6 mice and Cox4i1-GFP mice were used in our study. C57BL/6 mice and Cox4i1-GFP mice were provided by Cavens Biogle Model Animal Research Co., Ltd. (Suzhou, China) and Shanghai Model Organisms Center, Inc. respectively. All the mice were maintained on a 12-h light/dark cycle from 8 a.m. to 8 p.m. All animal studies were performed according to the guidelines evaluated and approved by the Animal Ethics Committee of Zhongshan hospital, Fudan University.

For acute experiments, 8-week-old mice was anesthetized with 2% isoflurane gas inhalation and performed with a single intraperitoneal injection of saline or doxorubicin (15 mg/kg). A total 50-100 μL of 1×10^5 mitochondria was transferred into the left ventricle with 3–4 injections by temporarily exteriorizing the heart through a left thoracic incision. After injecting mitochondria, the heart was carefully returned to the chest cavity with the help of a mosquito clamp. It was estimated that the mitochondria isolated from one mice heart could be transplanted into 10–15 mice heart. To calculate more clearly, about 1×10^6-2×10^6 Mitochondria could be collected from one mice heart. Then the number of mitochondria for transplantation to each mice was 1×10^5 Mitochondria. Actually, both the 1×10^6 and 1×10^5 mitochondria were explored in our previous study. The mice died within 5 min after injection of 1×10^6 mitochondria, some mice (around 30%–50%) died after injection of 5×10^5 mitochondria. All mice survived after 1×10^5 mitochondria injection, so this concentration was chosen. The control group was performed by injection of the same volume of normal saline. After injecting mitochondria, the heart was carefully returned to the chest cavity with the help of a mosquito clamp. To track the transplanted mitochondria, the mitochondria with GFP fluorescence were isolated from the hearts of Cox4i1-GFP mice. For the chronic experiment, 8-week-old mice were injected with doxorubicin (5 mg/kg) or normal saline once weekly for 4 weeks and followed by 4 dose-free weeks. DEX (50 mg/kg) was administered by intraperitoneal injection 2 h before doxorubicin injection once weekly for 4 weeks and followed by 4 dose-free weeks. The transplantation of mitochondria from mice heart and human arterial blood was conducted at the first two weeks in mice with chronic doxorubicin cardiotoxicity. The glutamine supplementation of doxorubicin (short and long term) administrated mice was maintained with or without 4% glutamine in their drinking water.

Human subject

The human arterial blood was collected from male patients of 40–50 age years old who were undergoing coronary angiogram due to coronary heart disease. These candidate patients were not involved in diabetes. The collection of arterial blood samples was approved by the Ethics Committee of Zhongshan hospital, Fudan University (ethical number: B2022-016R). Written informed consents were obtained from participants or their immediate families.

METHOD DETAILS

Cardiomyocyte isolation

The Langendorff-free method was used for the isolation of adult primary cardiomyocytes.[49] In brief, 8-week-old mice was anesthetized with pentobarbital (70 mg/kg) then the heart was perfused with 7mL high EDTA buffer in right ventricle to inhibit contraction and coagulation. After transferring into a dish, the heart was perfused with 10mL EDTA buffer and 3mL perfusion buffer in the apex of left ventricle. To deeply digest, the heart was injected with 30-40mL collagenase buffer into the apex of left ventricle. The disconnected cardiomyocytes were subsequently resuspended and plated onto a laminin-precoated culture dish (5 μg/mL) and maintained in a humidified culture incubator (Thermo Fisher Scientific, Waltham, MA, USA) under 5% CO2 at 37°C.

Doxorubicin treatment and mitochondrial transplantation of cultured cells

To perform doxorubicin treatment in cultured cells, H9C2 and adult primary cardiomyocytes were treated with 1μm M and 2μm M doxorubicin respectively for 24h. To perform *in vitro* mitochondrial transplantation into H9C2 and adult primary cardiomyocytes, the mitochondria were prepared by isolating from H9C2 and adult primary cardiomyocytes (donor cells). Then mitochondria were co-cultured with the corresponding receptors cells (the same number with donor cells) after doxorubicin treatment.

TEM staining assay

The fresh heart tissues were harvested and cut into small size of 1 mm3 in the glutaraldehyde. And then fixed with 1% OsO4 in 0.1M phosphate buffer (pH7.4) for 2h at room temperature. After removing OsO4, the tissues were rinsed in 0.1M phosphate buffer (pH7.4). After gradient dehydrating at room temperature, the sample were penetrated with resin and embed. The embedding models were polymerized at 65°C for more than 48h. And then the blocks were taken out from the embedding models for standby application at room temperature. The resin blocks were cut to 60-80nm thin and then fished out onto 150 meshes cuprum grids with formvar film. The cuprum grids were stained with 2% uranium acetate saturated alcohol solution and 2.6% Lead citrate. After drying overnight at room temperature, the cuprum grids were observed under TEM (HITACHI).

Mechanical function assay

Mechanical properties of cardiomyocytes were assessed using a SOFTEDGE MYOCAM system (IonOptix Corporation, Milton, MA, USA) as described previously.[26] Briefly, cardiomyocytes were isolated from control, doxorubicin and doxorubicin plus mitochondrial transfer groups, suspended with no BDM culture medium and dropped on the 24 × 24mm microscope cover glass under an inverted microscope (Olympus, IX-70). When stimulated by 0.5Hz frequency, the dynamic shorthening and relengthening properties of cardiomyocytes were recorded by IonOptix MyoCam camera. The cellular mechanical characteristics were analyzed by IONOPTIX SOFTEDGE software and demonstrated as the following indices: bl-resting cell length, dep v-maximal velocity of shortening (-dl/dt), dep vt-time to peak shortening (TPS-s), bl % peak h-peaking shortening (% cell lengthening), ret v:maximal velocity of relengthening (+dl/dt), t to bl 90.0%:Time to 90% relengthening (TR90-s).

Plasmid and siRNA transfection

Ogg1 plasmid and Gls siRNA was provided by Guangzhou RiboBio Co., Ltd. The lipofectamine 3000 reagent was used to transfect the Plasmid and siRNA according to the manufacturer's protocol. Briefly, the plasmid DNA-lipid/siRNA complexes were prepared and added into cells with 70–90% confluent.

Bioenergetics assay

In our study, the bioenergetics of cardiomyocytes in different treatment groups were evaluated by glycolysis and OXPHOS, which could be quantified by determining ECAR (ECAR) and the OCRs with an XFe96 extracellular flux analyzer (Seahorse Bioscience, Billerica, MA, USA) as described previously.[50] ECAR was determined by adding glucose(10mM), oligomycin A (1μM) and 2-deoxy-D-glucose(2-DG; 1M). And the metabolic profiles of OCR were detected by adding oligomycin A (1μM), 1μM FCCP, antimycin A (1μM) and rotenone (1μM).

Living cell imaging

Adult primary cardiomyocytes were isolated and cultured on costar 6 well plate. Then the mitochondria isolated from mouse heart were stained with Mitotracker green (Cell Signaling, Danvers, MA. USA) and incubated with cardiomyocytes after interfering with 2 μM doxorubicin. The cellular death and mitochondrial internalization were detected by living cell imaging analysis system (BioTek, Winooski, VT, USA).

Reactive oxygen species analysis

After Doxorubicin treatment or mitochondrial transplantation for about 24h, the cellular ROS levels was determined with DCFH-DA ROS assay kit (Mkbio, Shanghai, China). In brief, the probe of DCFH-DA was diluted at 1:1000 (5μM) and incubated with cardiomyocytes in the dark at 37°C for 30 min. Images with green fluorescence (λex = 488/λem = 525 nm) were then observed by a confocal microscope (Olympus, Japan). The mitochondrial ROS was detected by using by MitoSOX Red Superoxide Indicator (Invitrogen, Carlsbad, CA, USA). A working solution was

prepared by diluting the MitoSOX Red Superoxide Indicator with cellular culture medium with 1:2000. Cells were incubated with the working solution in a humidified culture incubator under 5% CO2 at 37°C for 10–15 min. Mitochondrial ROS was reflected by red fluorescence (λex = 510/λem = 580 nm) and captured by a fluorescence microscope (Olympus, Japan).

Mitochondria isolation from arterial blood

The arterial blood was collected from mice left ventricle and human radial artery respectively, the erythrocytes were subsequently lysed by lysing buffer (BD Biosciences, USA). Specifically, 10 times the volume of the lysing buffer was added into the arterial blood. Gently vortex each tube immediately and incubate at room temperature, protected from light, for 15 min. Then the tubes were centrifuged 3000X g for 10 min. The supernatant was carefully aspirated and repeat the above steps. Then mitochondria were isolated with a cellular mitochondria isolation kit (Beyotime Biotechnology, China) according to the manufacturer's protocol.

Briefly, the pellet resuspended in 0.5 mL mitochondria isolation buffer and grinded with three-dimensional freezing grinder under the frequency of 60 Hz. Then the tubes were centrifuged 600X g for 10 min. The mitochondrial solution was collected carefully without disturbing pellet. Finally, the mitochondria were obtained after centrifugation 600X g for 10 min. The isolated mitochondria were then counted by a Vi-cell XR system (Beckman coulter, Inc. USA).

Mitochondria isolation from mouse heart and cells

Mitochondria were isolated from mice heart and cultured H9C2 by using a tissue and cell mitochondrial isolation kit (Beyotime Biotechnology, China, Cat#C3606 and Cat#C3601) according to the manufacturer's instruction. The isolated mitochondria for transplantation were suspended and then quantized by a Beckman counter.

Echocardiography analysis

The cardiac function of mouse was acquired with a Vevo 2100 high-frequency ultrasound system (VisualSonics, Toronto, ON, Canada). Mice were anesthetized by isoflurane (3% for induction and 1.5% for maintenance), and M-mode images were measured and analyzed.

Mitotracker Green/deep red staining

For Mitotracker Green/deep red staining, the staining work solution was performed by diluting the Mitotracker deep red with cellular culture medium and incubated with cardiomyocytes for 20 min at 37°C. After incubation, the cells were imaged by a fluorescence microscope (Olympus, Japan).

TUNEL assay

The apoptotic cardiomyocytes were stained using One Step TUNEL Apoptosis Assay Kit (Beyotime Biotechnology, China). Nuclear counterstaining was performed with 4′,6-diamidino-2-phenylindole (DAPI, Beyotime Biotechnology, China), and the inflorescence staining of apoptotic cells were imaged by a fluorescence microscope (Olympus, Japan).

Tumor inhibition

To establish the mice tumor model, EMT6 cells (1×10^6) suspended in PBS were inoculated into the left flank of each Balb/c mice. When those tumors reached ~300 mm^3, animals were treated with saline, doxorubicin, doxorubicin and mitochondrial transplantation. Tumor volume was monitored by measuring the tumor diameter with caliper and the estimated volume was calculated. The image of the tumors was recorded at the end of treatment.

Total RNA extraction

Total RNA was extracted from the mouse heart using Trizol (Invitrogen, Carlsbad, CA, USA). The heart tissue was homogenized in Trizol for 2 min and then rested horizontally for 5 min. The supernatant was collected after centrifuging for 5 min at 12,000×g at 4°C, then transferred into chloroform/isoamyl alcohol (24:1). The mix was shacked vigorously for 15s, and then centrifuged at 12,000×g for 10 min at 4°C. After centrifugation, the upper aqueous phase was transferred into equal volume of supernatant of isopropyl alcohol, then centrifuged at 13,600 rpm for 20 min at 4°C. The RNA pellet was collected and washed twice with 1 mL 75% ethanol. In the end, the RNA pellet was obtained after air dry for 5–10 min, and then dissolved with DEPC-treated water. Nano Drop and Agilent 2100 bioanalyzer was used to quantify the RNA concentration (Thermo Fisher Scientific, MA, USA).

mRNA library construction

To obtain the cDNA, the mRNA was fragmented into small pieces. First-strand cDNA and second-strand cDNA synthesis was generated using random hexamer-primed reverse transcription. A-Tailing Mix and RNA Index Adapters were incubated with cDNA to end repair. The Ampure XP Beads were used to purify cDNA fragments, then dissolved in EB solution. The mRNA library was constructed after denaturing and circularizing the double stranded PCR products. The DNA nanoball (DNB) was obtained by amplifing with phi29 and loaded into the patterned nanoarray. Finally, pair end 100 bases reads were generated on BGIseq500 platform (BGI-Shenzhen, China).

Western blot analysis

Total protein of cells and myocardial tissue were extracted and separated by 10% and 12% sodium dodecyl sulfate polyacrylamide gel electrophoresis (SDS-PAGE), respectively, and then transferred to polyvinylidene difluoride (PVDF) membranes (Millipore, Burlington, CA, USA). After blocking with 5% bovine serum albumin (BSA) for 1 h, the membranes were incubated with primary antibodies at 4°C overnight and then horseradish peroxidase-conjugated secondary antibodies for 1 h at room temperature. The membranes were imaged using a Bio-Rad detection system (Bio-Rad Laboratories, Hercules, CA, USA). The primary antibody CS (Cat #14309S), VDAC (Cat #4661S), Bax (Cat #2772S), Bcl2 (Cat #3498S), TOM20 (Cat#42406S) and cleaved-caspase 3 (Cat #9662S) were obtained from Cell Signaling, Danvers, MA. NDUFAB1(Cat #ab181021), SDHD (Cat #ab189945), SDHA (Cat #ab137756), OGG1 (Cat #ab62826) and SOD2/MnSOD (Cat #ab68155) antibody were obtained from Abcam (MitoSciences-Abcam, Eugene, OR). GLS (also refers to KGA/GAC Polyclonal antibody) (Cat #12855-1-AP) antibody was obtained from Proteintech Group, Inc.

Flow cytometric analysis

Single-cell suspensions were prepared by using the multi-tissue dissociation kit 2 (Miltenyi Biotec). For cytometric analyses, the cells were incubated with a mixture of antibodies at 4°C for 20 min. The antibodies used in the present study are listed: FITC anti-mouse/human CD11b Antibody (BioLegend) (Cat#101206), PerCP/Cyanine5.5 anti-mouse CD45 Antibody (BioLegend) (Cat#103132), APC anti-mouse Ly-6G Antibody (BioLegend) (Cat#127614), Zombie Aqua Fixable Viability Kit (BioLegend) (Cat# 423102). The obtained results were expressed as the percent or cell number per microgram of tissue. Flow cytometric analysis and cell sorting were performed on an LSRFORTESSA and FACS Aria instruments (BD Biosciences, San Jose, CA, USA) and analyzed using FlowJo software (Tree Star).

Application of glutamine blockade

For *in vitro* study, cardiomyocytes were incubated with 1 μM DON for 24 h before harvesting for analyses. For *in vivo* study, JHU083 was dissolved in 2.5% ethanol in PBS (v/v) which was administered for all vehicle-treated control experiments. Mice were treated with JHU083 or vehicle by daily gavage with 1 mg/kg/day in 100 μL for days 6.[51]

Histology

Mice heart were fixed overnight in 4% paraformaldehyde, embedded in paraffin, and serially sectioned at 5-μm thickness. The sections were stained with Hematoxylin and Eosin (H&E) for routine histological examination with a light microscope. To measure collagen deposits, select sections were stained with Sirius red. For each mouse, three adjacent sections were quantified using ImageJ software (National Institutes of Health).

Metabolites extraction

All heart tissues were weighted and added extract solution (methanol, containing isotopically labeled internal standard mixture) in an EP tube. Then the samples were homogenized at 35 Hz for 4 min and sonicated for 5 min in ice-water bath. The homogenization and sonication cycle were repeated for 3 times. Then the samples were incubated for 1h at −40°C and centrifuged at 12000 rpm for 15 min at 4°C. The resulting supernatant was transferred to a fresh glass vial for analysis. The quality control sample was prepared by mixing an equal aliquot of the supernatants from all of the samples.

LC-MS/MS analysis

LC-MS/MS analyses were performed using an UHPLC system (Vanquish, Thermo Fisher Scientific) with a UPLC HSS T3 column (2.1 mm × 100 mm, 1.8 μm) coupled to Orbitrap Exploris 120 mass spectrometer (Orbitrap MS, Thermo). The mobile phase consisted of 5 mmol/L ammonium acetate and 5 mmol/L acetic acid in water (A) and acetonitrile (B). The auto-sampler temperature was 4°C, and the injection volume was 2 μL. The Orbitrap Exploris 120 mass spectrometer was used for its ability to acquire MS/MS spectra on information-dependent acquisition mode in the control of the acquisition software (Xcalibur, Thermo). In this mode, the acquisition software continuously evaluates the full scan MS spectrum. The ESI source conditions were set as following: sheath gas flow rate as 50 Arb, Aux gas flow rate as 15 Arb, capillary temperature 320°C, full MS resolution as 60000, MS/MS resolution as 15000 collision energy as 10/30/60 in NCE mode, spray Voltage as 3.8 kV (positive) or −3.4 kV (negative), respectively.

Data preprocessing and annotation of LC-MS/MS analysis

The raw data were converted to the mzXML format using ProteoWizard and processed with an in-house program, which was developed using R and based on XCMS, for peak detection, extraction, alignment, and integration. Then an in-house MS2 database (Biotree DB) was applied in metabolite annotation. The cutoff for annotation was set at 0.3.

QUANTIFICATION AND STATISTICAL ANALYSIS

Statistical analysis

Statistical analysis was performed using GraphPad Prism 8 (GraphPad Software Inc., San Diego, CA, USA) software, and data are presented as the mean ± standard error of mean (SEM). One-way ANOVA followed by Bonferroni's post-hoc test was applied for comparisons among multiple groups. Unpaired Student's t-tests were used for comparisons between two groups. All experiments were repeated at least three times. A p value less than 0.05 was considered to be statistically significant.